REMARKS

Applicants' representatives thank Examiner Davis and Primary Examiner Ungar for the interview of July 15, 2005. The amendments and remarks herein are made in accordance with our interview. Claims 44 and 56 are amended to delete the phrase "a chimeric antibody". Upon entry of the present amendments, claims 41-64 will be pending. No new matter has been added.

Deposit Requirement

The Examiner has maintained the request for an affidavit or declaration regarding the deposit. *See*, Paper No. 20050510, page 2. While applicants submit that the statement made in the response sent March 2, 2005 fully satisfies the requirements under the 37 C.F.R §§ 1.803-1.809, in accordance with the Examiner's request, the following declaration is respectfully submitted:

Availability of the Deposit

> Human Genome Sciences, Inc., the assignee of the present application, has deposited biological material under the terms of the Budapest Treaty on the International Recognition of the Deposit of Micro-organisms for the Purposes of Patent Procedure with the following International Depository Authority: American Type Culture Collection (ATCC), 10801 University Boulevard, Manassas, Virginia 20110-2209 (present address). The deposit was made on October 11, 1994, accepted by the ATCC, and given ATCC Accession Number 75913. In accordance with M.P.E.P. § 2410.01 and 37 C.F.R. § 1.808, assurance is hereby given that all restrictions on the availability to the public of ATCC Accession Number 75913 will be irrevocably removed upon the grant of a patent based on the instant application, except as permitted under 37 C.F.R. § 1.808(b). The assignee of the present application will replace the deposited biological material should the deposited material be destroyed or rendered non-viable.

In view of the above affirmation and explanation, attested to by the signature (below) of the Attorney for the Applicants, it is respectfully requested that the rejection of claim 53 under 35 U.S.C. § 112, first paragraph, be withdrawn.

Rejection of Claims 44 and 56 under 35 U.S.C. §112, second paragraph

The Examiner has maintained the rejection of claims 44 and 56 under 35 U.S.C. § 112, second paragraph as allegedly being indefinite for the use of the language "a chimeric antibody". *See*, Paper No. 20050510, page 3. Applicants have amended claims 44 and 56 to

remove the objected language. Accordingly this rejection has been obviated and should be withdrawn.

Rejection of Claims 41-64 under 35 U.S.C. § 112, first paragraph

The Examiner has maintained the rejection of claims 41-64, under 35 U.S.C § 112, first paragraph, for lack of enablement. *See*, Paper No. 20050510, pages 3-8. More specifically, the Examiner alleges that "it is not predictable that one could use the claimed polypeptide for detecting metastasized prostate cells, because it is unpredictable that metastasized prostate cells still express the claimed sequence". See *id.*

Applicants respectfully disagree and traverse.

Preliminarily, Applicants point out that the pending claims are directed to methods of detecting prostatic specific reductase (PSR) protein using PSR specific antibodies and thus do not require the PSR proteins to have a particular recited utility. Accordingly, in order to fully enable the claimed methods as required by 35 U.S.C. § 112, the proteins detected according to the claimed methods need only have a single use (e.g., as an enzymatic reductase), and the specification need only enable a person of ordinary skill in the art to practice the claimed methods without undue experimentation.[1]

Applicants submit that the enzymatic reductase activity of PSR protein is a specific, substantial and credible use. Additionally, one of ordinary skill in the art, when armed with the disclosure of the specification, would require no more than routine experimentation to practice the claimed methods. Therefore, Applicants assert that the claimed methods are fully enabled irrespective of, for example, the expression profile of PSR protein in normal and metastasized prostate tissue.

The specification discloses that PSR protein has enzymatic activity as a reductase. *See, e.g.*, last sentence in paragraph 2. The reductase activity of the PSR protein, first identified by Applicants and disclosed in the instant application, is corroborated by the post-filing disclosures of Lin *et al.*, (*Cancer Research* 61:1611-1618 (2001); submitted as Reference AR in Applicants' Information Disclosure Statement of December 19, 2001 and resubmitted herewith as Exhibit A) and Kedishvili *et al*, (*Journal Biological Chemistry* 277(32):28909-28915 (2002); attached herewith as Exhibit B). As noted in Applicants' reply

[1] Applicants need to show utility for only one disclosed purpose. See Raytheon Co. v. Roper Corp., 220 USPQ 592 (Fed. Cir. 1983, *cert denied*, 469 U.S. 835 (1984); Ex parte Lanham, 121 USPQ 223 (Pat Off. Bd. App. 1958).

sent March 2, 2005, the PSR protein disclosed in the present application and the PSDR1 protein disclosed in Lin *et al.*, share greater than 98% sequence identity (see e.g., alignment submitted in Applicants' reply sent March 2, 2005, and resubmitted herewith as Exhibit C). As can be seen in Figure 2 of Lin *et al.* (page 1615) and in the alignment provided in Exhibit C, PSR and PSDR1 both contain the conserved sequence segments (i.e., GlyXXXGlyXGly and TyrXXXLys), which are present in members of the short-chain dehydrogenase/reductase enzyme family. *See* Figure 2 legend of Lin et al. for conserved sequence segments. Furthermore, the minor sequence differences between PSR and PSDR1 do not appear to be at positions conserved amongst the portions of the proteins aligned in Figure 2 of Lin *et al.* Accordingly, Lin *et al.*, support the proposition that PSR and PSDR1 have the same enzymatic activity, despite having minor sequence differences.

As further support, Kedishvili *et al.* demonstrate that PSDR1 has reductase activity (*See, e.g.*, abstract). Thus, the publications of Lin *et al.* and Kedishvili *et al.* corroborate that PSR has enzymatic activity as a reductase.

Applicants respectfully submit that the enzymatic reductase activity of PSR is specific, substantial, and credible. Moreover, the skilled artisan, enlightened by the teaching of the present specification and the high level of skill in the art, would be more than capable of routinely making and using an antibody that specifically binds the PSR protein to routinely practice the claimed methods of detecting PSR protein.

Furthermore, Applicants reemphasize that the relevant legal inquiry with respect to enablement of the pending claims is not whether the antibodies used according to the claimed methods would bind and therefore detect variant PSR proteins, but rather whether the claimed methods involving use of antibodies that specifically bind the polypeptides of SEQ ID NO:2 or ATCC Deposit No. 75913 to detect PSR in a biological sample can be confirmed, without undue experimentation, by following procedures either described in the specification or otherwise known in the art. For the reasons stated above, Applicants submit that the claimed methods are fully enabled.

In summary, Applicants submit that due to: (1) the availability of routine methods in the art for generating antibodies; (2) the availability of routine methods for detecting the presence of PSR protein; (3) the teachings in the specification and the corroborating evidence that PSR is an enzymatic reductase; and (4) the high level of skill in the field of immunology and molecular biology, one skilled in the art could routinely generate antibodies and then use these antibodies to detect PSR protein and thus satisfy the limitations recited in the claims.

In light of the above remarks, it is clear that the specification as originally filed fully enables the claimed methods. Accordingly, Applicants respectfully request that the rejection of claims 41-64, under 35 U.S.C. § 112, first paragraph, for lack of enablement, be reconsidered and withdrawn.

CONCLUSION

Applicants respectfully request that the above remarks be made of record in the file history of the instant application. Applicants respectfully submit that the present application is now in condition for allowance. A Notice of Allowance is earnestly solicited. If, in the opinion of the Examiner, a telephone conference would expedite prosecution, the undersigned can be reached at the telephone number indicated below.

No fee is believed to be due in connection with this filing, however if applicants are in error, please charge any fee deemed necessary to Deposit Account No. 08-3425.

Dated: September 23, 2005

Respectfully submitted,

By _____
Kenley K. Hoover
Registration No.: 40,302
HUMAN GENOME SCIENCES, INC.
Intellectual Property Dept.
14200 Shady Grove Road
Rockville, Maryland 20850
(301) 610-5771

KKH/PF/ba

[CANCER RESEARCH Vol. 61, 1611–1618, February 15, 2001]

Prostate Short-Chain Dehydrogenase Reductase 1 (*PSDR1*): A New Member of the Short-Chain Steroid Dehydrogenase/Reductase Family Highly Expressed in Normal and Neoplastic Prostate Epithelium[1]

Biaoyang Lin, James T. White, Camari Ferguson, Shunyou Wang, Robert Vessella, Roger Bumgarner, Lawrence D. True,[5] Leroy Hood,[6] and Peter S. Nelson[2]

Departments of Molecular Biotechnology [B. L., J. T. W., P. S. N.], Medicine [P. S. N.], Urology [S. T., R. V.], Microbiology [R. B.], and Pathology [L. D. T.], University of Washington, Seattle, Washington 98195, the Institute for Systems Biology, Seattle, Washington 98103 [L. H.], and the Division of Human Biology, Fred Hutchinson Cancer Research Center, Seattle, Washington 98109 [C. F., P. S. N.]

ABSTRACT

Genes regulated by androgenic hormones are of critical importance for the normal physiological function of the human prostate gland, and they contribute to the development and progression of prostate carcinoma. We used cDNA microarrays comprised of prostate-derived cDNAs to profile transcripts regulated by androgens in prostate cancer cells. This study identified a novel gene that we have designated prostate short-chain dehydrogenase/reductase 1 (*PSDR1*), that exhibits increased expression on exposure to androgens in the LNCaP prostate cancer cell line. Northern analysis demonstrated that *PSDR1* is highly expressed in the prostate gland relative to other normal human tissues. The *PSDR1* cDNA and putative protein exhibit homology to the family of short-chain dehydrogenase/reductase enzymes and thus identify a new member of this family. Cloning and analysis of the putative *PSDR1* promoter region identified a potential androgen-response element. We used a radiation-hybrid panel to map the *PSDR1* gene to chromosome 14q23-24.3. *In situ* hybridization localizes *PSDR1* expression to normal and neoplastic prostate epithelium. These results identify a new gene involved in the androgen receptor-regulated gene network of the human prostate that may play a role in the pathogenesis of prostate carcinoma.

INTRODUCTION

Prostate adenocarcinoma is responsible for more than 39,000 deaths annually in the United States (1). Circulating androgens and the intracellular AR[3] are critical mediators of prostate cancer growth and the progression to lethal disease. Landmark discoveries by Huggins and Hodges in 1941 (2) demonstrated that most prostate cancers are initially androgen-dependent, a finding that initiated the era of effective endocrine-based therapy for this malignancy. To date, surgical or chemical castration remains the mainstay of therapy for advanced prostate cancer. A reduction in serum testosterone leads to marked tumor regression through a mechanism of programmed cell death (3). Although responses to this therapy may last for years, the approach is rarely curative because surviving cancer cells lose their dependency on exogenous testosterone over time and are capable of proliferating in the absence of detectable serum androgens.

In addition to a role in driving cellular proliferation, an intact androgen signaling system may also be associated with tumor suppression (4). This dual role of androgens would not be unexpected, because androgens are responsible for differentiation of the prostate epithelium and for the regulation of specific epithelial cell functions such as the expression of PSA (5, 6). Several androgen-regulated genes have been demonstrated to be associated with a proliferative shut-off function in LNCaP cells and for the regulation of the cell cycle (7, 8). At the time of invasion or metastasis, mutations in the AR may occur (9), suggesting that a normal AR is protective from progression. Finally, *in vitro* studies indicate that there may be a survival advantage in maintaining an androgen-responsive cohort of prostate tumor cells (10). This concept has been extended to clinical medicine in which several trials suggest a benefit for an approach using intermittent rather than continuous androgen suppression in patient cohorts with hormone-responsive disease (11, 12).

The pivotal role of androgens in the biology and treatment of prostate cancer has led to intensive investigations designed to identify the molecular mediators of androgen action (13, 14). Among the genes shown to be regulated by androgens in prostate cells are several that encode enzymes belonging to the two major lipogenic pathways: fatty acid synthesis and cholesterol synthesis (15, 16). The regulation of cholesterol metabolism by androgens is especially intriguing because cholesterol is an essential precursor for the biosynthesis of androgens (17). Other molecules involved in androgen metabolism and androgen action are themselves androgen regulated. For example, 17-β-HSD, an enzyme that converts androstenedione to testosterone, is androgen regulated (18), as is the expression of the AR itself (7, 19). It appears that multiple autoregulatory levels of androgen action may be operative in androgen-responsive tissues.

Our objective in this study was to identify genes that exhibit transcriptional regulation by androgens in human prostate cells. We hypothesized that such genes could be direct mediators of androgen action and that the characterization of these genes and their cognate proteins would provide insights into the mechanisms of androgen-dependent and androgen-independent cellular growth. We used cDNA microarrays comprised of cDNAs derived from human prostate tissues to quantitate transcripts expressed in the androgen-sensitive LNCaP prostate tumor cell line under conditions of androgen starvation or androgen stimulation. Here we report the cDNA cloning, chromosomal mapping, genomic structure, and expression profile of a novel gene, *PSDR1*, that exhibits homology to the family of SDR enzymes. *PSDR1* is the first SDR shown to be predominantly expressed in normal and neoplastic prostate tissue. We hypothesize that *PSDR1* may play a role in steroid hormone metabolism in prostate cells and thus may be an ideal target for modulating hormone-mediated prostate cancer growth.

MATERIALS AND METHODS

Microarray Fabrication. A nonredundant set of 1500 prostate-derived cDNA clones were identified from the Prostate Expression DataBase (PEDB), a public genetic repository of EST data derived from human prostate cDNA

Received 6/7/00; accepted 12/13/00.

The costs of publication of this article were defrayed in part by the payment of page charges. This article must therefore be hereby marked "*advertisement*" in accordance with 18 U.S.C. Section 1734 solely to indicate this fact.

[1] Supported in part by the CaPCURE Foundation, by Grant CA75173-01A1 from the National Cancer Institute (NIH) (to P. S. N.), and by gifts from the Seattle Foundation and the Lazar Foundation.

[2] To whom requests for reprints should be addressed, at the Division of Human Biology, Fred Hutchinson Cancer Research Center, Mailstop D4-100, 1100 Fairview Avenue North, Seattle, Washington 98109-1024. E-mail: pnelson@fhcrc.org.

[3] The abbreviations used are: AR, androgen receptor; PSA, prostate-specific antigen; ARE, androgen response element; DHT, dihydrotestosterone; EST, expressed sequence tag; dbEST, database of ESTs; CS-FCS, charcoal-stripped FCS; PRE, progesterone responsive element; HSD, hydroxysteroid dehydrogenase; RACE, rapid amplification of cDNA ends; SDR, short-chain dehydrogenase reductase; PSDR1, prostate SDR 1; hs, human glandular kallikrein.

libraries (20). Individual clone inserts were amplified by the PCR using 2 µl of bacterial transformant culture as template with primers BL_m13F (5'-CTAAAACGACGGCCAGTGAATTG-3') and BL_m13R (5'-ACACAGGAAACAGCTATGACCATG-3' as described previously (21). PCR products were purified through Sephacryl S500 (Pharmacia), mixed 1:1 with DMSO (Amersham), and spotted in duplicate onto coated type IV glass microscope slides (Amersham) using a Molecular Dynamics GenII robotic spotting tool. After spotting, the glass slides were air-dried and UV-cross-linked with 500 mJ of energy and then baked at 95°C for 30 min.

Probe Construction and Microarray Hybridization. Total RNA was isolated from LNCaP cells after 72 hrs of androgen depletion or supplementation using TRIzol (Life Technologies) according to the manufacturer's directions. Fluorescence-labeled probes were made from 30 µg total RNA in a reaction volume of 20 µl containing 1 µl of anchored oligo-dT primer (Amersham), 0.05 mm Cy3-dCTP or Cy5-dCTP (Amersham); 0.05 mm dCTP; 0.1 mm each dGTP, dATP, dTTP, and 200 units of Superscript II reverse transcriptase (Life Technologies). Reactants were incubated at 42°C for 120 min followed by heating to 94°C for 3 min. Unlabeled RNA was hydrolyzed by the addition of 1 µl of 5 N NaOH and heating to 37°C for 10 min. One µl of 5 M HCl and 5 µl of 1 M Tris-HCl (pH 7.5) were added to neutralize the base. Unincorporated nucleotides and salts were removed by chromatography (Qiagen), and the cDNA was eluted in 30 µl of dH_2O. One µg of dA/dT 12–18 (Pharmacia) and 1 µg of human Cot1 DNA (Life Technologies) were added to the probe, heat denatured at 94°C for 5 min, combined with an equal volume of 2× microarray hybridization solution (Amersham), and prehybridized at 50°C for 1 h. The mixture was then placed onto a microarray slide with a coverslip and hybridized in a humid chamber at 52°C for 16 hours. The slides were washed once with 1× SSC, 0.2% SDS at room temperature for 5 min, then twice with 0.1× SSC, 0.2% SDS at room temperature for 10 min. After washing, the slides were rinsed in distilled water to remove trace salts and dried.

Image Acquisition and Data Analyses. Fluorescence intensities of the immobilized targets were measured using a laser confocal microscope (Molecular Dynamics). Intensity data were integrated at a pixel resolution of 10 µm using ~20 pixels per spot, and recorded at 16 bits. Quantitative data were obtained with the SpotFinder V 2.4 program written at the University of Washington. Local background hybridization signals were subtracted prior to comparing spot intensities and determining expression ratios. For each experiment, each cDNA was represented twice on each slide, and the experiments were performed in duplicate producing four data points per cDNA clone per hybridization probe. Intensity ratios for each cDNA clone, hybridized with probes derived from androgen-stimulated LNCaP and androgen-starved LNCaP, were calculated (stimulated intensity/starved intensity). Gene-expression levels were considered significantly different between the two conditions if all four of the replicate spots for a given cDNA demonstrated a ratio >2 or <0.5, and the signal intensity was greater than 2 SD above the image background.

Cell Culture and General Methods. DNA manipulations including transformation, plasmid preparation, gel electrophoresis, and probe labeling, were performed according to standard procedures (22). The LNCaP prostate carcinoma cell line was cultured in RPMI 1640 supplemented with 10% FCS (Life Technologies, Rockville, MD). Cells were transferred into RPMI 1640 with 10% CS-FCS (Life Technologies) 24 h before androgen-regulation experiments. This medium was replaced with fresh CS-FCS media or CS-FCS supplemented with 1 nM synthetic androgen R1881 (NEN Life Science Products Inc.). Cells were harvested for RNA isolation at 0-h and 72-h time points.

Northern Analysis. Ten µg of total RNA were fractionated on 1.2% agarose denaturing gels and transferred to nylon membranes by a capillary method (22). The human multiple tissue and master blots were obtained from Clontech. Blots were hybridized with DNA probes labeled with [α-^{32}P]dCTP by random priming using the Rediprime II random primer labeling system (Amersham) according to the manufacturer's protocol. Filters were imaged and quantitated by using a phosphor-capture screen and Image-quant software (Molecular Dynamics).

cDNA Library Screening and RACE. We screened 1,200,000 phage plaques from a human prostate 5'-stretch cDNA library (Clontech) with the 6A4 cDNA probe representing the 3' end of the *PSDR1* cDNA. Two separate rounds of library screening identified 16 partial-length cDNA clones. Searches of dbEST identified seven IMAGE cDNA clones (IMAGE CloneID, 360400, 109237, 1130518, 1401718, 1337270, 1723130, 1703429) that contained sequences homologous to *PSDR1*. All of the clones were sequenced and assembled using the Sequencher software (Gene Codes, Corp.). To clone the 5' end of the cDNA, 5'-RACE was performed on human prostate Marathon-Ready cDNA (Clontech) using primers 6A3_RC3 (5'-GGACAGCATTTTCCTGATTTGGGGC-3') and 6A4_RC4 (5'-CAGAAGGAGGAGCAACAGCGGGAAC-3'). The RACE products were subcloned into PCR2.1-TOPO (Invitrogen) and sequenced.

Phage plaques (1,200,000) from a human prostate 5'-STRETCH cDNA library (Clontech) were screened with *PSDR1* ^{32}P-cDNA probes according to the manufacturer's instructions. Eleven additional cDNA clones were isolated, subcloned and sequenced. RACE reactions were performed using the human prostate Marathon-ready cDNA cloning kit (Clontech) following the manufacturer's instructions. Templates for RACE reactions were prostate Marathon-ready cDNA (Clontech) and androgen-stimulated LNCaP cDNA prepared using Marathon cDNA amplification kit (Clontech). Nested 5'-RACE reactions were performed according to the manufacturer's instructions; first with primers 6A4RC4, 5'-CAGAAGGAGGAGCAACAGCGGGAAC-3' and AP1 (Clontech) and then a nested RACE reaction with primers 6A4RC3, 5'-GGACAGCATTTTCCTGATTTGGGGC-3' and AP2 (Clontech). The RACE products were subcloned into PCR2.1-TOPO vectors with the TOPO TA cloning kit (Invitrogen) and sequenced.

Chromosomal Localization of *PSDR1* by Radiation Hybrid Panel Mapping. The G3 Gene bridge radiation hybrid panel (Research Genetics, Huntsville, AL) was used to map the chromosomal localization of *PSDR1* with primers 6A4F (5'-GCGGCATTTCCTTACATTGTCTTG-3') and 6A4R (5'-CACTCCAACAAGTGATGGGAACAC-3'). After 35 cycles of amplification, the reaction products were separated on a 1.2% agarose gel, and the resulting product pattern was analyzed through the Stanford genome center web server* to determine the probable chromosomal location.

***In Situ* Hybridization.** For mRNA *in situ* hybridization, recombinant plasmid pCR2.1-TOPO (Invitrogen), containing a 400-bp *PSDR1* fragment was linearized to generate sense and antisense digoxigenin-labeled RNA probes. *In situ* hybridization was performed according to the manufacturer's protocol on the Ventana GenII automated instrument (Ventana Medical Systems, Tucson, AZ). Tissue sections (5 µm) were mounted onto Chroma plus slides (VWR Scientific), deparaffinized in a 65°C oven for 2 h followed by three 5-min soaks in xylene and rehydrated through graded alcohol with a final rinse in 2× SSC. Before hybridization, sections were digested with protease 1 cocktail for 12 min at 37°C, then 10 ng of either sense or antisense probe in the hybridization buffer was applied. Programmed recipe files consisting of buffer rinses, protease digestion, hybridization, detection, and counterstains were optimized for the *PSDR1* probe. Digoxigenin-labeled RNA probe was added manually. Antidigoxigenin was used as the primary antibody. The probe was denatured at 65°C, and hybridization was carried out at 42°C for 360 min. Washes were performed at 37°C with 2×, 1×, and 0.1× SSC. The system uses a cocktail of antirabbit and antimouse secondary IgG-biotinylated antibody with an indirect biotin-avidin diaminobenzidine detection system. The sections were counterstained with hematoxylin.

RESULTS

Identification of a Novel Androgen-regulated cDNA, *PSDR1*, by Microarray Expression Analysis. Microarrays comprised of cDNA clones derived from prostate tissues were hybridized with total cDNA probes synthesized from androgen-stimulated and androgen-starved LNCaP prostate cancer cells. Four independent data points for each arrayed cDNA were generated. The hybridization ratios for 20 distinct cDNAs were consistently increased by >2-fold in androgen-stimulated relative to androgen-starved cells. We did not observe any cDNAs with consistent hybridization ratios <0.5, a ratio that would indicate down-regulated expression. The genes induced by androgens included *hK2* (23), *hK3*, also known as PSA (24), *NKX3.1* (25), *prostate/PRSS17* (26), *TMPRSS2* (13), *PART-1* (27), several genes involved in lipid metabolism, and several anonymous ESTs. The expression level of

* Internet address: http://shgc.stanford.edu.

the cDNA clone corresponding to one of these ESTs, 6A4, increased 3-fold in androgen-stimulated LNCaP cells relative to androgen-deprived cells as assayed by microarray hybridization (Fig. 1*A*). Sequence comparisons against the GenBank and dbEST databases revealed homology only to uncharacterized partial-length ESTs (*e.g.*, AA657851, IMAGE ID:1207405). Full-length cloning of the corresponding cDNA and subsequent nucleotide and amino acid sequence comparisons revealed significant homology to conserved motifs of the SDR family of proteins. We have named this gene *PSDR1* for Prostate Short-chain Dehydrogenase/Reductase 1.

Cloning of the Full-Length *PSDR1* cDNA. We screened a human prostate cDNA library with the 6A4 cDNA probe representing the 3' end of the *PSDR1* cDNA and identified 16 partial-length cDNA clones. Searches of the dbESTs initially identified seven IMAGE cDNA clones (IMAGE Clone ID 360400, 109237, 1130518, 1401718, 1337270, 1723130, 1703429) that contained sequence homologous to *PSDR1*. To clone the 5' end of the cDNA, 5'-RACE was performed on cDNA from normal human prostate (Clontech) and the LNCaP cell line. All of the clones were sequenced and subsequently assembled using the Sequencher software (Gene Codes, Corp.). A total of 25[illegible]9 bp were obtained, which corresponds to the 2.5-kb band

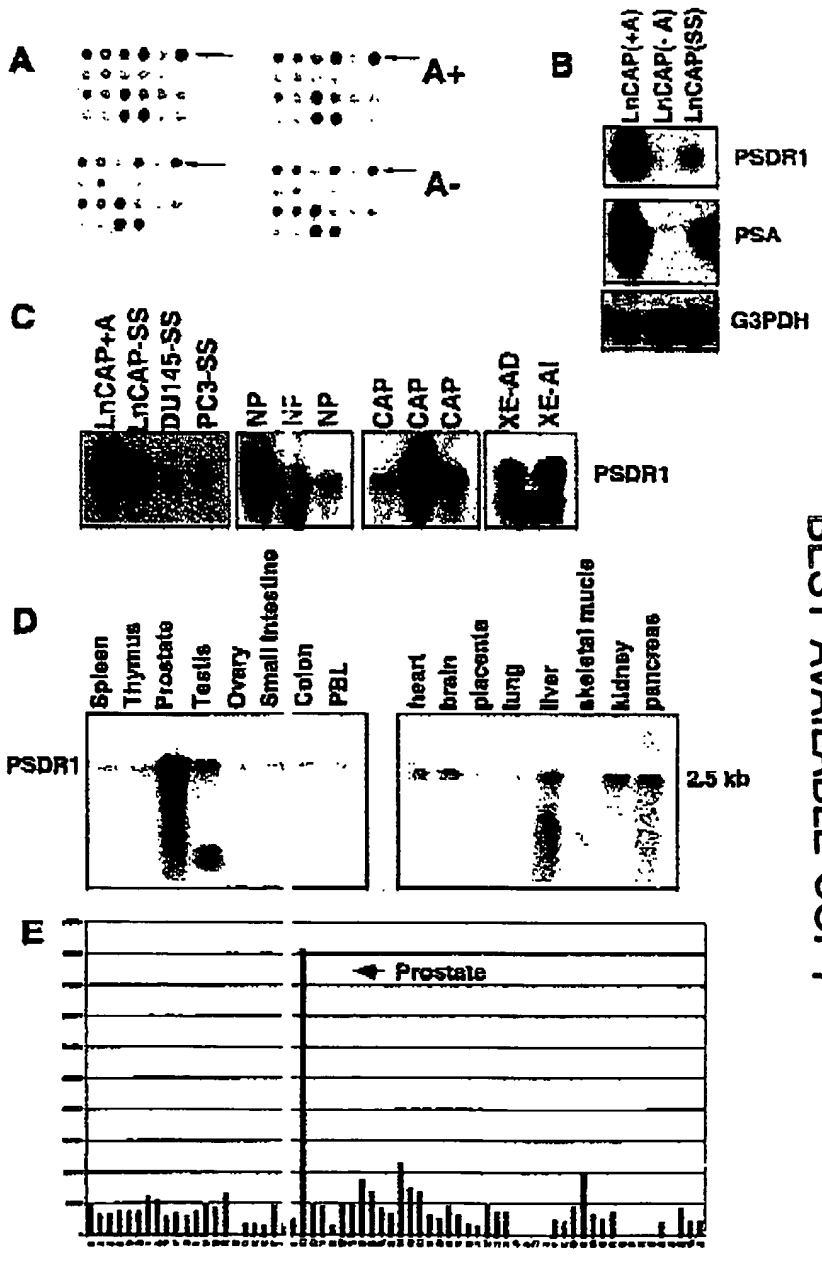

Fig. 1 *A*, a representative microarray hybridization section showing the androgen-stimulated expression of PSDR1 cDNAs from androgen-stimulated (+v) and androgen starved (+−) LNCaP cells were labeled and hybridized to cDNA microarrays. *Arrows*, the location of PSDR1 cDNA on the microarray. *B*, Northern analysis of the same RNAs used in the microarray experiment hybridized with PSDR1, PSA, and G3PDH probes. *LNCaP(SS)*, LNCaP cells at steady state grown in 10% serum without additional androgens and harvested at 70% confluence. *C*, Northern analysis demonstrating PSDR1 expression in the prostate cancer cell lines LNCaP, DU145, and PC3 grown in 10% serum (*SS*) or with additional androgen (+*A*), three normal prostate tissue samples (*NP*), three primary prostatic adenocarcinoma samples (*CAP*) and androgen-dependent (*XE-AD*) and androgen-independent xenografts (*XE-AI*). *D*, Northern analysis demonstrating the PSDR1 expression profile in normal human tissues. *E*, a multiple tissue dot blot (Clontech) containing 50 human tissue RNAs was hybridized with PSDR1 probe. Signal intensities were captured with phosphor screen and scanned with a phosphorimager. *Bar graph*, signal intensities calculated with ImageQuant program. The 50 human tissues are *A1*, whole brain, *A2*, amygdala, *A3*, caudate nucleus, *A4*, cerebellum, *A5*, cerebral cortex, *A6*, frontal lobe, *A7*, hippocampus, *A8*, medulla oblongata, *B1*, occipital lobe, *B2*, putamen, *B3*, substantia nigra, *B4*, temporal lobe, *B5*, thalamus, *B6*, accumens, *B7*, spinal cord, *C1*, heart, *C2*, aorta, *C3*, skeletal muscle, *C4*, colon, *C5*, bladder, *C6*, uterus, *C7*, prostate, *C8*, stomach, *D1*, testis, *D2*, ovary, *D3*, pancreas, *D4*, pituitary gland, *D5*, adrenal gland, *D6*, thyroid gland, *D7*, salivary gland, *D8*, mammary gland, *E1*, kidney, *E2*, liver, *E3*, small intestine, *E4*, spleen, *E5*, thymus, *E6*, peripheral leukocyte, *E7*, lymph node, *E8*, bone marrow, *F1*, appendix, *F2*, lung, *F3*, trachea, *F4*, placenta, *G1*, fetal brain, *G2*, fetal heart, *G3*, fetal kidney, *G4*, fetal liver, *G5*, fetal spleen, *G6*, fetal thymus, *G7*, fetal lung, *H1*, yeast total RNA, *H2*, yeast tRNA, *H3*, E Coli rRNA, *H4*, *Escherichia coli* DNA, *H5*, poly r(A), *H6*, human C$_0$t 1 DNA, *H7*, human DNA, *H8*, human DNA. B8, F5–F8 and G8 contain no RNAs. The units on the *Y* axis are relative intensity units.

which is in agreement with the size of its transcript as determined by Northern hybridization (Fig. 1*D*). The cDNA sequence was submitted to GenBank under the accession no. AF167438.

The *PSDR1* cDNA encodes a putative protein of 318 amino acids. The start codon, GAGATGG matches in a strong context to the Kozak translation initiation consensus sequences (RNNATGG, where R is a purine; Ref. 28). Two potential polyadenylation signals were identified at nucleotide positions 2439 and 2481. IMAGE clone 1703429 has a poly(A) stretch that uses the AATAAA polyadenylation signal at 2419, and our original cDNA clone 6A4 uses the AATAAA signals at 2481. However, we were not able to find a polyadenylation site that would produce the 900-bp band seen in testis tissue. PCR primers flanking the start and stop codons were designed, and an expected size band encompassing the entire coding region was amplified from human prostate Marathon-Ready cDNA (Clontech, data not shown).

Comparisons of the assembled cDNA sequences indicated several polymorphic sites. Five distinct single nucleotide polymorphisms were recognized between the three independent prostate tissue sources used for *PSDR1* cloning. Three occur in the coding region of the *PSDR1* sequence; nucleotide 379, ggc to ggg, nucleotide 916, gtg to gtc; and nucleotide 921, gtc to gcc. The first two are conserved changes, whereas the latter results in a valine to alanine amino acid substitution. Alignments of sequences in dbEST with homology to *PSDR1* identified more than 20 distinct nucleotide differences in tissue sources presumably derived from different individuals.

Prostate-localized and Androgen-regulated Expression of *PSDR1*. The androgen-regulated expression of *PSDR1* was confirmed by Northern analysis using the same LNCaP RNA that was used for microarray analysis. PhosphorImage quantitation of the Northern analysis demonstrated a 3-fold induction of *PSDR1* expression after 72 h of androgen exposure relative to 72 h of androgen starvation (Fig. 1*B*). PSA expression increased 25-fold, and the expression of the G3PDH loading control did not change significantly. Interestingly, Northern analysis with androgen-independent prostate cancer cell lines DU145 and PC3 demonstrated *PSDR1* expression in both cell types (Fig. 1*C*) indicating a mechanism of *PSDR1* transcription in these cells that is independent of androgen requirements.

The distribution of *PSDR1* transcripts in normal human tissues and prostate carcinoma was determined by Northern analysis and mRNA dot blot. Of 16 adult tissues examined by Northern, a *PSDR1* message of 2.5 kb was predominantly expressed in prostate (Fig. 1*D*). In testis, the *PSDR1* probe hybridized to an additional band at about 900 bp (Fig. 1*D*), which could indicate cross-hybridization, alternate splicing, or alternate usage of polyadenylation signals. The *PSDR1* expression profile was confirmed using an RNA Master dot blot (Clontech) comprised of RNA from 50 different tissues. *PSDR1* expression was detected predominantly in prostate with a very low relative level of expression in spleen, thymus, testis, ovary, small intestine, colon, peripheral blood leukocyte, and kidney, adrenal gland, and fetal liver (Fig. 1*E*). *PSDR1* expression was at least 4-fold higher in prostate relative to any other human tissue examined. *PSDR1* expression was detected in all of the normal and neoplastic prostate tissue samples examined. These included three normal whole prostate tissues; three primary prostate adenocarcinomas, androgen-dependent and androgen-independent prostate cancer xenografts, and three prostate cancer cell lines (Fig. 1*C*).

PSDR1 Shares Homology with Members of the SDR Family. We used the nucleotide and translated the 318-amino acid *PSDR1* sequence to search the National Center for Biotechnology Information sequence databases by using BLAST and BEAUTY algorithms (29). Partial homology was seen with several oxidoreductases from bacteria and plant sources. To see whether the homology was significant, we searched the protein sequence of *PSDR1* against the BLOCKS database (30).[3] The *PSDR1* protein has three blocks that all match to the SDR family protein signature BLOCK (BL00061; Ref. 31) with a significant combined E-value of 2.6e-06. The SDR family are NAD- or NADP-dependent oxidoreductases (31), which include enzymes involved in steroid metabolism such as estradiol 17-β-dehydrogenase (also called 17-β-hydroxysteroid dehydrogenase, EC 1.1.1.62), 15-hydroxyprostaglandin dehydrogenase (NAD+) (EC 1.1.1.141) from human and 11 β-HSD (EC 1.1.1.146, 11-DH; Ref. 31). A multiple sequence alignment of the *PSDR1* protein with different members of the human HSD family and a prokaryotic 20-β-HSD (Streptomyces 3α/20β-HSD) is shown in Fig. 2.

Only two motifs are highly conserved in the SDR family. The first is a common GlyXXXGlyXGly pattern, in which the coenzyme NAD(H) or NADP(H) binds at the NH_2 terminus of the SDR enzyme (31). The second motif is a segment, TyrXXXLys, believed to be involved in the catalytic activity of the enzyme (32). The *PSDR1* protein contains these two signatures (as shown by *asterisk* in Fig. 2). Sequence alignments reveal that proteins in the SDR family exhibit residue identities of only about 15–30%, probably because of their early divergence and remote origin (31). *PSDR1* shows ~25% amino acid identity with other members of the SDR family.

Searches against prosite patterns database[4] revealed that *PSDR1* contains two Asn-glycosylation sites at amino acid (aa) position 174 and 198. These two sites are also conserved among SDR family proteins (Fig. 2). In addition, two protein kinase C (PKC) phosphorylation sites (aa 57 and 106), a casein kinase II phosphorylation site (aa 57), and a 7 *N*-myristoylation site are identified in the protein.

***PSDR1* Genomic Organization and Promoter Sequence Analysis.** BLAST searches with the full-length *PSDR1* cDNA identified homology with nucleotide sequence derived from a recently deposited unannotated 197-kb chromosome 14 BAC clone, R-1012A1, sequenced by the National Sequencing Center-Genoscope in France (GenBank accession no. AL049779). Alignment with the *PSDR1* sequence demonstrated that this BAC contains the entire *PSDR1* cDNA and allowed for the determination of the *PSDR1* genomic structure. The *PSDR1* gene comprises 7 exons and 6 introns. The sizes of exons and introns and the exon/intron junctional sequences are listed in Fig. 3*B*. All of the intron/exon junctions conform to the 5′-gt...3′-ag consensus (33) except intron 2. Intron 2 has a 5′-gc...3′-ag splicing signal, a structure that has been identified in other genes (34).

We examined the 5′ genomic sequences for potential transcriptional start sites using a neural network promoter prediction program[7] (35) and for potential transcriptional factor binding site using the TESS (Transcription Element Search Software) program[8] (36). We identified a strong promoter sequence with a score of 0.87 (a score of 0.85 has a 0.1–0.4% false positive prediction rate). The predicted transcription start site is 167 bp 5′ of the ATG start codon. A TATA box (TATAAT) is found 30 bp 3′ of the putative transcriptional initiation site (Fig. 3*A*). A sequence that has 86.7% homology (13 of 15 nucleotides) to the consensus ARE, 5′-GGA/TACAnnnTGTTCT-3′, (37) was identified (Fig. 3*A*). Two sequences that have 86.7% (13 of 15 nucleotides) homology to the consensus sequence of PREs (38) were also identified (Fig. 3*A*). An interleukin-6 response element binding protein site, TTCCCAGAA, (39) was identified 281 bp 5′ of the transcription initiation site.

Chromosomal Localization of *PSDR1*. The medium-resolution Stanford G3 radiation hybrid panel was used to determine the chro-

[3] Internet address: http://www.blocks.fhcrc.org.
[4] Internet address: http://www.isrec.isb-sib.ch/software/PFSCAN_form.html
[7] Internet address: http://www-hgc.lbl.gov/projects/promoter.html
[8] Internet address: http://www.cbil.upenn.edu/tess/index.html

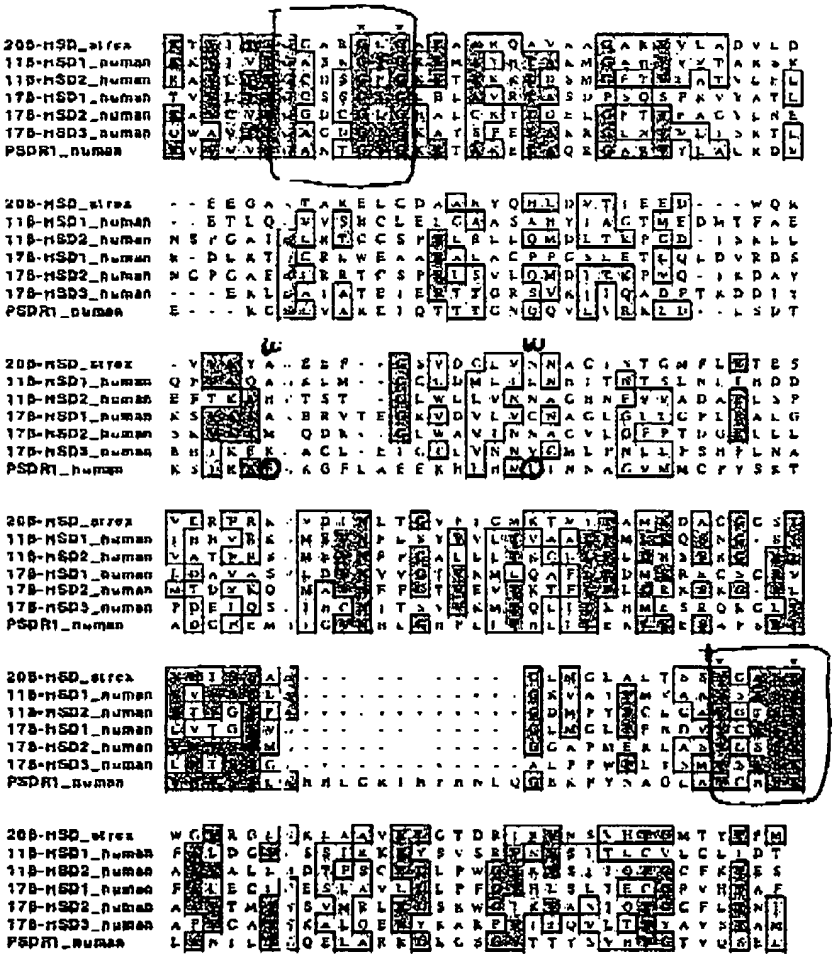

Fig. 2. Multiple sequence alignments of PSDR1 with different members of the human HSDs from the SDR family. A prokaryotic 20 β-HSD (Streptomyces 3α/20β-HSD) was included at the top (*20-β HSD_strep*). The alignment was performed with the ClustalW algorithm (36) using MacVector 6.0 software (Oxford Molecular). BLOSUM series matrix was used with an open-gap penalty score of 10 and extend-gap penalty score of 0.05. *Boxed* and *dark-shaded*, identical residues; *boxed* and *light-shaded*, similar residues. *, two conserved segments of the SDR family, GlyXXXGlyXGly and TyrXXXLys. The GenBank accession numbers for members aligned here are 20-β HSD_Strep, Streptomyces 3α/20β-HSD, P19992; 11-β HSD1_human, P28845; 11-β HSD2_human, U14631; 17-β-HSD1_human, P14061; 17-β-HSD2_human, L11708; 17-β-HSD3_human, P37058. Only the regions containing the conserved motifs are shown here.

inosomal localization of *PSDR1* using gene-specific PCR primers 6A4F and 6A4R. Analysis of the typing results on the Stanford Human Genome Center Radiation Hybrid Panel server[*] indicated that *PSDR1* is located closest to Stanford Human Genome Center Radiation Hybrid Panel-2558 between two cytogenetically mapped markers D4S63 (mapped to 14q23) and D4S258 (mapped to 14q24.3).[*] Therefore, *PSDR1* is mapped to 14q23-24.3, consistent with the BAC clone mapping data localizing *BAC R-10I2A1* to chromosome 14q.

***PSDR1* Expression in Normal and Neoplastic Prostate Epithelium.** Normal prostate contains two major epithelial cell populations, the luminal secretory cells and the basal cells. *In situ* hybridizations were performed on sections of normal prostate by using an antisense RNA probe specific for *PSDR1* to localize its expression. *PSDR1* was expressed in both normal basal and luminal cell populations (Fig. 4 *A* and *C*). Little to no staining was seen in fibromuscular stromal cells, endothelial cells, or infiltrating lymphocytes. Hybridization with sense *PSDR1* RNA probes showed no background staining (Fig. 4, *B* and *D*). *In situ* hybridizations with *PSDR1* antisense and sense probes were also performed on sections of primary prostate adenocarcinoma obtained from radical prostatectomy specimens. Adenocarcinoma cells were uniformly positive for *PSDR1* expression (Fig. 4*E*). Hybridization with sense *PSDR1* RNA probes showed no background staining (Fig. 4*F*).

DISCUSSION

In a search for genes regulated by androgens in the human prostate, we have identified a new member of the SDR superfamily. SDRs encompass a large group of functionally diverse proteins in pro- and eukaryotes (31). Enzymes in this family typically exhibit residue identities of only 15–30%, indicating early gene duplication events and subsequent extensive divergence (31). Regions of high conservation are restricted to specific segments, which indicate a possible common fold, active site, reaction mechanism, and coenzyme and substrate binding regions (30). Of relevance for the study of androgen-mediated effects in prostate carcinoma is the classification of several key enzymes involved in steroid biosynthesis, HSDs, within the SDR family. This group of HSDs includes 17-β-HSD types 1–4 and 6 (41), 15-hydroxyprostaglandin dehydrogenase, and 11-β-HSD (31). 17-β-HSD 3 converts androstenedione to testosterone (42), 17-β-HSD 6 converts 3-androstane-3α, 17-β-diol (3-adiol) to androsterone (43). In prostate cancer cells, 17-β-HSD type 2 exclusively converts 5α-DHT and testosterone into the less potent 17-keto compounds 5α-androstanedione and 4-androstenedione, respectively (44). This suggests

[*] The Genome Database, http://www.gdb.org/.

that 17HSD type 2 plays a part in the androgen metabolic pathway, resulting in the inactivation of testosterone and 5α-DHT locally in the prostate. Enzyme expression in the prostate could, therefore, protect cells from excessive androgen action. Because *PSDR1* shows significant homology to HSD members of the SDR family, we hypothesize that *PSDR1* is also involved in prostate cellular steroid metabolism that may include biosynthesis and/or degradation. The pharmacological modulation of *PSDR1* activity could thus influence prostate cellular growth and provide a new target for prostate cancer therapy.

Numerous studies support associations between molecular variations involving genes of the androgen metabolic pathway and the development and progression of prostate cancer (45). In addition to environmental influences, racial and international variation in prostate cancer incidence suggests that inheritable genetic factors such as those that influence androgen biosynthesis, activation, transport, and metabolism are operative (45). In addition to polymorphic variation in the AR itself (46), specific polymorphisms in the 5α-reductase type 2 (*SRD5A2*) gene, the enzyme converting testosterone to the more bioactive DHT, result in increased enzyme activity and confer up to a 7-fold increased risk for the development of prostate cancer in African-American men (47). Allelic variants in the *3-β-HSD type II* gene, encoding one of two enzymes that initiates the inactivation of DHT, have been identified and are currently under assessment for a role in racial/ethnic differences in prostate carcinogenesis (48). Polymorphisms in *PSDR1* could influence enzyme activity and consequently result in variations in steroid metabolism between individuals. Our preliminary analysis of the *PSDR1* sequence from three different prostate tissue sources identified five distinct single nucleotide polymorphisms. Three occur in the coding region of the *PSDR1* sequence, one of which results in a valine to alanine amino acid substitution. An alignment of sequences in dbEST with homology to *PSDR1* identified more than 20 distinct nucleotide differences in tissue sources presumably derived from different individuals. Although some of these differences may represent sequencing artifacts, these findings warrant a more directed study of *PSDR1* variation in different ethnic populations and in samples of prostate carcinoma.

A. Schematic of the PSDR1 promoter region

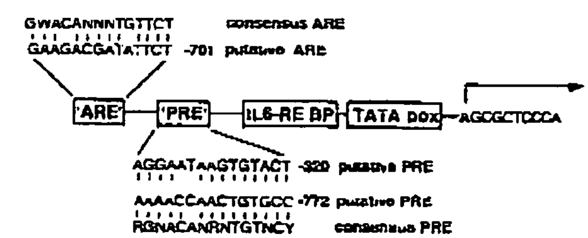

B. Summary of the genomic structure of PSDR1

Exon	Acceptor	Donor	Exon size	Intron size (bp)
1	–	CAG[illegible]	>114	2977
2	[illegible]cagCAA	GAG[illegible]	130	340
3	[illegible]cagGAG	GAG[illegible]	159	1193
4	[illegible]cagGAA	TGG[illegible]	104	718
5	[illegible]cagGTC	AAG[illegible]	2?1	5007
6	[illegible]cagGCT	CAG[illegible]	191	6691
7	[illegible]cagTGA	–	1621	–

Fig. 3. Genomic structure of PSDR1. *A*, schematic drawing showing the putative sequence motifs of the PSDR1 promoter. Arrow, the predicted transcription initiation site. *A*, the +1 putative TATAAT *TATA*-box at −30, putative ARE and PRE sequences, and an interleukin-6 response element binding protein *IL-6 RE-BP* site TTCCCAGAA at −261 are also shown. IUPAC-IUB codes for nucleotides were used: *R*, purine; *Y*, pyrimidine; *W*, A or T; *B*, not A (C, G, or T); *K*, G or T; *M*, A or C; *N*, any nucleotide. *B*, PSDR1 exon and intron acceptor and donor splice sites with corresponding segment sizes in nucleotide base pairs.

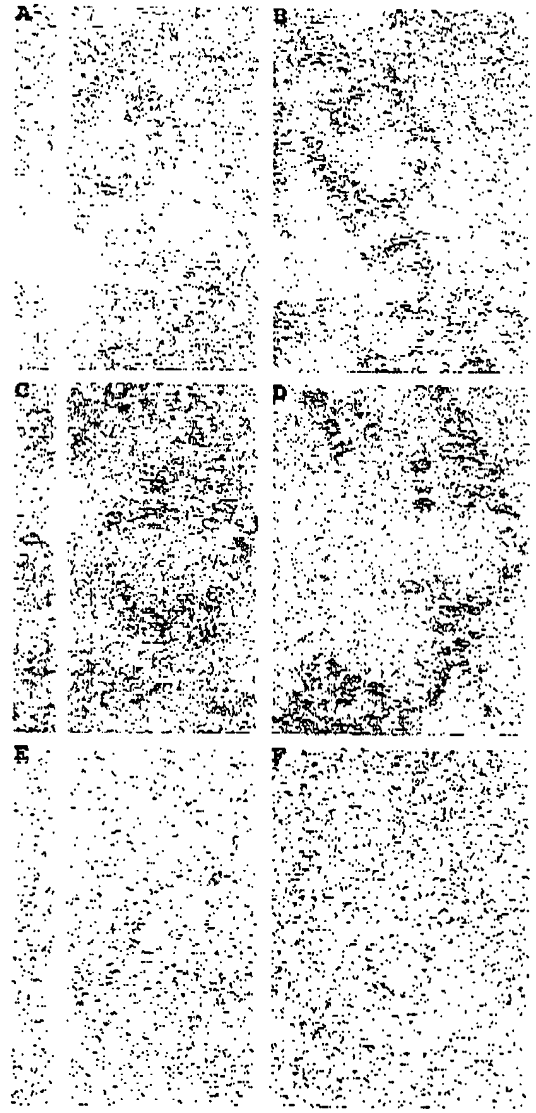

Fig. 4. Representative sections of *in situ* hybridization with PSDR1 probes in normal and malignant prostate tissues. Low (*A*) and high (*C*) power magnification of normal prostate tissue hybridized with PSDR1 antisense probe, showing expression in both basal and luminal cells, but not in stromal cells. Low (*B*) and high (*D*) power magnification of negative control hybridization with PSDR1 sense probes, showing no background staining in normal prostate tissue. *E*, primary prostate carcinoma tissue hybridized with PSDR1 antisense probe showing PSDR1 expression in prostate carcinoma cells. *F*, negative control hybridization with PSDR1 sense probes, showing no background tissue hybridization.

The expression of *PSDR1* is induced by synthetic androgens in LNCaP cells. The mechanism of androgen-mediated regulation of *PSDR1* expression is unknown and could involve either direct AR binding to *PSDR1* promoter regions or indirect activation through the modulation of intermediary transcription factors or via posttranscriptional mechanisms. Androgens have been shown to regulate expression of other oxidoreductases. The mouse alcohol dehydrogenase *ADH1*, which belongs to the long-chain dehydrogenase family, is induced 10–12 fold by androgens in mouse kidney cells (49). The induction of mouse *ADH1* gene by androgens seems to be AR de-

pendent because the *ADH1* gene in *Tfm* mice lacking functional AR was not responsive to androgens (49). 17-β-HSD1, which belongs to the SDR family, is stimulated by androgen through AR-mediated mechanism (50). We have identified a putative ARE and two putative PRE sites that demonstrate a high degree of homology to the respective consensus hormone receptor binding sites. Whether these responsive elements are functional awaits further investigation. In addition, *PSDR1* transcription is not entirely mediated by androgens as demonstrated by a low level of detectable *PSDR1* message in androgen-starved LNCaP cells and in the androgen-independent PC3 and DU145 prostate cancer cell lines. Studies of the *PSDR1* protein may identify additional mechanisms of functional regulation.

The localized expression of *PSDR1* in prostate epithelium is interesting because, to our knowledge, *PSDR1* is the first member of the human SDR family that is expressed predominantly in the prostate gland. Other members of SDR family exhibit tissue-restricted patterns of expression. For example, 17-β-HSD1 is predominantly expressed in placenta and ovary (51, 52); 17-β-HSD2 is expressed in placenta and liver (53); 17-β-HSD3 is expressed in testis (42); 17-β-HSD4 is primarily expressed in liver and kidney (54), 17-β-HSD5 is expressed most abundantly in liver and testis (41, 55), and 17-β-HSD6 is expressed equally in liver and prostate (43).

The identification of genes with selective expression in specific organs or cell types provides an entry point for understanding biological processes that occur uniquely within a particular tissue. Genes and their cognate proteins whose expression is specific for the prostate have greatly aided the diagnosis and treatment of prostate carcinoma. The significance of the prostate predominant expression pattern of *PSDR1* remains to be determined. If the tissue expression profile of the *PSDR1* protein corresponds to the transcript expression profile, then *PSDR1* may represent an additional target for prostate cancer diagnostic and therapeutic interventions. Cellular or humoral immunotherapy could be designed to exploit the tissue expression differential. Our hypothesis is that *PSDR1* is involved in steroid synthesis and/or degradation in normal and neoplastic prostate epithelium, and, as such, it may be a key enzyme involved in maintaining intracellular balance of steroid hormones in these cells. Additional studies including the expression of *PSDR1* protein and the analysis of substrate specificity and kinetics are needed to address this question.

ACKNOWLEDGMENTS

We thank Steve Lasky, John Hall, and the Molecular Biotechnology Sequencing Facility for DNA sequencing support.

REFERENCES

1. Landis, S. H., Murray, T., Bolden, S., and Wingo, P. A. Cancer statistics, 1999. CA Cancer J. Clin., 49: 8–31, 1999.
2. Huggins, C. and Hodges, C. V. Studies on prostate cancer I. The effect of castration, of estrogen and of androgen injection on serum phosphatases in metastatic carcinoma of the prostate. Cancer Res., 1: 293–297, 1941.
3. Denmeade, S. R., Lin, X. S., and Isaacs, J. T. Role of programmed (apoptotic) cell death during the progression and therapy for prostate cancer (published erratum appears in Prostate, 28: 414, 1996). Prostate, 28: 251–265, 1996.
4. Prehn, R. T. On the prevention and therapy of prostate cancer by androgen administration. Cancer Res., 59: 4161–4164, 1999.
5. Bonkhoff, H., Stein, U., and Remberger, K. Multidirectional differentiation in the normal, hyperplastic, and neoplastic human prostate: simultaneous demonstration of cell-specific epithelial markers. Hum. Pathol., 25: 42–46, 1994.
6. Bonkhoff, H., and Remberger, K. Differentiation pathways and histogenetic aspects of normal and abnormal prostatic growth: a stem cell model. Prostate, 28: 98–106, 1996.
7. Geck, P., Szelei, J., Jimenez, J., Lin, T. M., Sonnenschein, C., and Soto, A. M. Expression of novel genes linked to the androgen-induced, proliferative shutoff in prostate cancer cells. J. Steroid Biochem. Mol. Biol., 63: 211–218, 1997.
8. Kokontis, J. M., Hay, N., and Liao, S. Progression of LNCaP prostate tumor cells during androgen deprivation: hormone-independent growth, repression of proliferation by androgen, and role for p27Kip1 in androgen-induced cell cycle arrest. Mol. Endocrinol., 12: 941–953, 1998.
9. Marcelli, M., Ittmann, M., Mariani, S., Sutherland, R., Nigam, R., Murthy, L., Zhao, Y., DiConcini, D., Puxeddu, E., Esen, A., Eastham, J., Weigel, N. L., and Lamb, D. J. Androgen receptor mutations in prostate cancer. Cancer Res., 60: 944–949, 2000.
10. Sato, N., Gleave, M. E., Bruchovsky, N., Rennie, P. S., Goldenberg, S. L., Lange, P. H., and Sullivan, L. D. Intermittent androgen suppression delays progression to androgen-independent regulation of prostate-specific antigen gene in the LNCaP prostate tumour model. J. Steroid Biochem. Mol. Biol., 58: 139–146, 1996.
11. Grossfeld, G. D., Small, E. J., and Carroll, P. R. Intermittent androgen deprivation for clinically localized prostate cancer: initial experience. Urology, 51: 137–144, 1998.
12. Crook, J. M., Szumacher, E., Malone, S., Huan, S., and Segal, R. Intermittent androgen suppression in the management of prostate cancer. Urology, 53: 530–534, 1999.
13. Lin, B., Ferguson, C., White, J. T., Wang, S., Vessella, R., True, L. D., Hood, L., and Nelson, P. S. Prostate-localized and androgen-regulated expression of the membrane-bound serine protease TMPRSS2. Cancer Res., 59: 4180–4184, 1999.
14. Gregory, C. W., Hamil, K. G., Kim, D., Hall, S. H., Pretlow, T. G., Mohler, J. L., and French, F. S. Androgen receptor expression in androgen-independent prostate cancer is associated with increased expression of androgen-regulated genes. Cancer Res., 58: 5718–5724, 1998.
15. Swinnen, J. V., and Verhoeven, G. Androgens and the control of lipid metabolism in human prostate cancer cells. J. Steroid Biochem. Mol. Biol., 65: 191–198, 1998.
16. Swinnen, J. V., Van Veldhoven, P. P., Esquenet, M., Heyns, W., and Verhoeven, G. Androgens markedly stimulate the accumulation of neutral lipids in the human prostatic adenocarcinoma cell line LNCaP. Endocrinology, 137: 4468–4474, 1996.
17. Norman, A. W., and Litwack, G. Steroid hormones: chemistry, biosynthesis, and metabolism. In: Hormones, Ed. 2, pp. 49–86. Academic Press, San Diego, California, 1997.
18. Zhou, Z., and Speiser, P. W. Regulation of HSD17B1 and SRD5A1 in lymphocytes. Mol. Genet. Metab., 68: 410–417, 1999.
19. Burnstein, K. L., Maiorino, C. A., Dai, J. L., and Cameron, D. J. Androgen and glucocorticoid regulation of androgen receptor cDNA expression. Mol. Cell. Endocrinol., 115: 177–186, 1995.
20. Hawkins, V., Doll, D., Bumgarner, R., Smith, T., Abajian, C., Hood, L., and Nelson, P. S. PEDB: the Prostate Expression Database. Nucleic Acids Res., 27: 204–208, 1999.
21. Nelson, P. S., Ng, W. L., Schummer, M., True, L. D., Liu, A. Y., Bumgarner, R. E., Ferguson, C., Dimak, A., and Hood, L. An expressed-sequence-tag database of the human prostate: sequence analysis of 1168 cDNA clones. Genomics, 47: 12–25, 1998.
22. Sambrook, J., Fritsch, E. F., and Maniatis, T. Molecular Cloning. Cold Spring Harbor, NY: Cold Spring Harbor Laboratory Press, 1989.
23. Murtha, P., Tindall, D. J., and Young, C. Y. Androgen induction of a human prostate-specific kallikrein, hKLK2: characterization of an androgen response element in the 5′ promoter region of the gene. Biochemistry, 32: 6459–6464, 1993.
24. Young, C. Y., Montgomery, B. T., Andrews, P. E., Qui, S. D., Bilhartz, D. L., and Tindall, D. J. Hormonal regulation of prostate-specific antigen messenger RNA in human prostatic adenocarcinoma cell line LNCaP. Cancer Res., 51: 3748–3752, 1991.
25. Bieberich, C. J., Fujita, K., He, W. W., and Jay, G. Prostate-specific and androgen-dependent expression of a novel homeobox gene. J. Biol. Chem., 271: 31779–31782, 1996.
26. Nelson, P. S., Gan, L., Ferguson, C., Moss, P., Gelinas, R., Hood, L., and Wang, K. Molecular cloning and characterization of prostase, an androgen-regulated serine protease with prostate-restricted expression. Proc. Natl. Acad. Sci. USA, 96: 3114–3119, 1999.
27. Lin, B., White, J. T., Ferguson, C., Bumgarner, R., Friedman, C., Trask, B., Ellis, W., Lange, P., Hood, L., and Nelson, P. S. *PART-1*, a novel human prostate-specific, androgen-regulated gene that maps to chromosome 5q12. Cancer Res., 60: 858–863, 2000.
28. Kozak, M. An analysis of 5′-noncoding sequences from 699 vertebrate messenger RNAs. Nucleic Acids Res., 15: 8125–8148, 1987.
29. Altschul, S. F., Gish, W., Miller, W., Myers, E. W., and Lipman, D. J. Basic local alignment search tool. J. Mol. Biol., 215: 403–410, 1990.
30. Pietrokovski, S., Henikoff, J. G., and Henikoff, S. The Blocks database—a system for protein classification. Nucleic Acids Res., 24: 197–200, 1996.
31. Jornvall, H., Persson, B., Krook, M., Atrian, S., Gonzalez-Duarte, R., Jeffery, J., and Ghosh, D. Short-chain dehydrogenases/reductases (SDR). Biochemistry, 34: 6003–6013, 1995.
32. Ghosh, D., Pletnev, V. Z., Zhu, D. W., Wawrzak, Z., Duax, W. L., Pangborn, W., Labrie, F., and Lin, S. X. Structure of human estrogenic 17-β-hydroxysteroid dehydrogenase at 2.20 Å resolution. Structure, 3: 503–513, 1995.
33. Breathnach, R., and Chambon, P. Organization and expression of eucaryotic split genes coding for proteins. Annu. Rev. Biochem., 50: 349–383, 1981.
34. Devireddy, L. R., and Jones, C. Alternative splicing of the latency-related transcript of bovine herpesvirus 1 yields RNAs containing unique open reading frames. J. Virol., 72: 7294–7301, 1998.
35. Reese, M. G., Harris, N., and Eeckman, F. Large scale sequencing specific neural networks for promoter and splice site recognition. In: Biocomputing: Proceedings of the 1996 Pacific Symposium. Singapore: World Scientific Publishing Corp., 1996.
36. Schug, J., and Overton, G. TESS: Transcription element search software on the WWW. Computational Biology and Informatics Laboratory, School of Medicine, University of Pennsylvania, Philadelphia, 1997.
37. Roche, P. J., Hoare, S. A., and Parker, M. G. A consensus DNA-binding site for the androgen receptor. Mol. Endocrinol., 6: 2229–2235, 1992.

38. Lieberman, B. A., Bona, B. J., Edwards, D. P., and Nordeen, S. K. The constitution of a progesterone response element. Mol. Endocrinol., 7: 515–527, 1993.
39. Hocke, G. M., Barry, D., and Fey, G. H. Synergistic action of interleukin-6 and glucocorticoids is mediated by the interleukin-6 response element of the rat α2 macroglobulin gene. Mol. Cell. Biol., 12: 2282–2294, 1992.
40. Persson, B., Krook, M., and Jornvall, H. Characteristics of short-chain alcohol dehydrogenases and related enzymes. Eur. J. Biochem., 200: 537–543, 1991.
41. Dufort, I., Rheault, P., Huang, X. F., Soucy, P., and Luu-The, V. Characteristics of a highly labile human type 5 17-β-hydroxysteroid dehydrogenase. Endocrinology, 140: 568–574, 1999.
42. Geissler, W. M., Davis, D. L., Wu, L., Bradshaw, K. D., Patel, S., Mendonca, B. B., Elliston, K. O., Wilson, J. D., Russell, D. W., and Andersson, S. Male pseudohermaphroditism caused by mutations of testicular 17-β-hydroxysteroid dehydrogenase 3. Nat. Genet., 7: 34–39, 1994.
43. Biswas, M. G., and Russell, D. W. Expression cloning and characterization of oxidative 17β- and 3α-hydroxysteroid dehydrogenases from rat and human prostate. J. Biol. Chem., 272: 15959–15966, 1997.
44. Elo, J. P., Akinola, L. A., Poutanen, M., Vihko, P., Kyllonen, A. P., Lukkarinen, O., and Vihko, R. Characterization of 17-β-hydroxysteroid dehydrogenase isoenzyme expression in benign and malignant human prostate. Int. J. Cancer, 66: 37–41, 1996.
45. Ross, R. K., Pike, M. C., Coetzee, G. A., Reichardt, J. K., Yu, M. C., Feigelson, H., Stanczyk, F. Z., Kolonel, L. N., and Henderson, B. E. Androgen metabolism and prostate cancer: establishing a model of genetic susceptibility. Cancer Res., 58: 4497–4504, 1998.
46. Stanford, J. L., Just, J. J., Gibbs, M., Wicklund, K. G., Neal, C. L., Blumenstein, B. A., and Ostrander, E. A. Polymorphic repeats in the androgen receptor gene: molecular markers of prostate cancer risk. Cancer Res., 57: 1194–1198, 1997.
47. Makridakis, N. M., Ross, R. K., Pike, M. C., Crocitto, L. E., Kolonel, L. N., Pearce, C. L., Henderson, B. E., and Reichardt, J. K. Association of mis-sense substitution in *SRD5A2* gene with prostate cancer in African-American and Hispanic men in Los Angeles, USA. Lancet, 354: 975–978, 1999.
48. Devgan, S. A., Henderson, B. E., Yu, M. C., Shi, C. Y., Pike, M. C., Ross, R. K., and Reichardt, J. K. Genetic variation of 3β-hydroxysteroid dehydrogenase type II in three racial/ethnic groups: implications for prostate cancer risk. Prostate, 33: 9–12, 1997.
49. Felder, M. R., Watson, G., Huff, M. O., and Ceci, J. D. Mechanism of induction of mouse kidney alcohol dehydrogenase by androgen. Androgen-induced stimulation of transcription of the *Adh-1* gene. J. Biol. Chem., 263: 14531–14537, 1988.
50. Couture, P., Theriault, C., Simard, J., and Labrie, F. Androgen receptor-mediated stimulation of 17β-hydroxysteroid dehydrogenase activity by dihydrotestosterone and medroxyprogesterone acetate in ZR-75-1 human breast cancer cells. Endocrinology, 132: 179–185, 1993.
51. Peltoketo, H., Isomaa, V., Maentausta, O., and Vihko, R. Complete amino acid sequence of human placental 17-β-hydroxysteroid dehydrogenase deduced from cDNA. FEBS Lett., 239: 73–77, 1988.
52. Peltoketo, H., Isomaa, V., Poutanen, M., and Vihko, R. Expression and regulation of 17-β-hydroxysteroid dehydrogenase type 1. J. Endocrinol., 150 (Suppl.): S21–S30, 1996.
53. Wu, L., Einstein, M., Geissler, W. M., Chan, H. K., Elliston, K. O., and Andersson, S. Expression cloning and characterization of human 17-β-hydroxysteroid dehydrogenase type 2, a microsomal enzyme possessing 20 α-hydroxysteroid dehydrogenase activity. J. Biol. Chem., 268: 12964–12969, 1993.
54. Adamski, J., Normand, T., Leenders, F., Monte, D., Begue, A., Stehelin, D., Jungblut, P. W., and de Launoit, Y. Molecular cloning of a novel widely expressed human 80 kDa 17-β-hydroxysteroid dehydrogenase IV. Biochem. J., 311: 437–443, 1995.
55. Lin, H. K., Jez, J. M., Schlegel, B. P., Peehl, D. M., Pachter, J. A., and Penning, T. M. Expression and characterization of recombinant type 2 3 α-hydroxysteroid dehydrogenase (HSD) from human prostate: demonstration of bifunctional 3α/17-β-HSD activity and cellular distribution (published erratum appears in Mol. Endocrinol., 12: 1763, 1998). Mol. Endocrinol., 11: 1971–1984, 1997.
56. Thompson, J. D., Higgins, D. G., and Gibson, T. J. CLUSTAL W: improving the sensitivity of progressive multiple sequence alignment through sequence weighting, position-specific gap penalties and weight matrix choice. Nucleic Acids Res., 22: 4673–4680, 1994.

Exhibit 5

THE JOURNAL OF BIOLOGICAL CHEMISTRY
© 2002 by The American Society for Biochemistry and Molecular Biology, Inc

Vol. 277, No. 32, Issue of August 9, pp. 28909–28915, 2002
Printed in U.S.A.

Evidence That the Human Gene for Prostate Short-chain Dehydrogenase/Reductase (*PSDR1*) Encodes a Novel Retinal Reductase (RalR1)*

Received for publication, March 18, 2002, and in revised form, May 24, 2002
Published, JBC Papers in Press, May 29, 2002, DOI 10.1074/jbc.M202588200

Natalia Y. Kedishvili‡§, Olga V. Chumakova‡, Sergei V Chetyrkin‡¶, Olga V. Belyaeva‡, Elena A. Lapshina‡, Daniel W. Lin‖, Masazumi Matsumura**, and Peter S. Nelson**‡‡**

*From the ‡Division of Molecular Biology and Biochemistry, School of Biological Sciences, University of Missouri-Kansas City, Kansas City, Missouri 64110, the Departments ‖Urology and ‡‡Medicine, University of Washington, Seattle, Washington 98195, and the **Division of Human Biology, Fred Hutchinson Cancer Research Center, Seattle, Washington 98109*

All-*trans*-retinoic acid is a metabolite of vitamin A (all-*trans*-retinol) that functions as an activating ligand for a family of nuclear retinoic acid receptors. The intracellular levels of retinoic acid in tissues are tightly regulated, although the mechanisms underlying the control of retinoid metabolism at the level of specific enzymes are not completely understood. In this report we present the first characterization of the retinoid substrate specificity of a novel short-chain dehydrogenase/reductase (SDR) encoded by *RalR1*/*PSDR1*, a cDNA recently isolated from the human prostate (Lin, B., White, J. T., Ferguson, C., Wang, S., Vessella, R., Bumgarner, R., True, L. D., Hood, L., and Nelson, P. S. (2001) *Cancer Res.* 61, 1611–1618). We demonstrate that RalR1 exhibits an oxidoreductive catalytic activity toward retinoids, but not steroids, with at least an 800-fold lower apparent K_m values for $NADP^+$ and NADPH *versus* NAD^+ and NADH as cofactors. The enzyme is ~50-fold more efficient for the reduction of all-*trans*-retinal than for the oxidation of all-*trans*-retinol. Importantly, RalR1 reduces all-*trans*-retinal in the presence of a 10-fold molar excess of cellular retinol-binding protein type I, which is believed to sequester all-*trans*-retinal from nonspecific enzymes. As shown by immunostaining of human prostate and LNCaP cells with monoclonal anti-RalR1 antibodies, the enzyme is highly expressed in the epithelial cell layer of human prostate and localizes to the endoplasmic reticulum. The enzymatic properties and expression pattern of RalR1 in prostate epithelium suggest that it might play a role in the regulation of retinoid homeostasis in human prostate.

All-*trans*-retinoic acid is a metabolite of vitamin A (all-*trans*-retinol) that functions as an activating ligand for a family of nuclear retinoic acid receptors (1). In target tissues, all-*trans*-retinoic acid is produced by the oxidation of all-*trans*-retinal-dehyde catalyzed by cytosolic aldehyde dehydrogenases (Fig. 1) (2–5). Retinaldehyde, in turn, can be produced either by the oxidation of retinol catalyzed by microsomal or cytosolic retinol dehydrogenases (reviewed in Refs. 6 and 7) or by a symmetrical cleavage of β-carotene (Fig. 1) (8). In the small intestine, the majority of absorbed β-carotene is converted directly to all-*trans*-retinal by cytosolic β,β-carotene 15,15′-dioxygenase (9). All-*trans*-retinal produced from β-carotene is reduced to all-*trans*-retinol by microsomal retinal reductase activity (10). The enzyme that catalyzes this reaction in the small intestine functions in the presence of cellular retinol binding protein type II (CRBPII),[1] which is expressed specifically in the small intestine and binds all-*trans*-retinal with high affinity (K_d of ~100 nM) (11). Retinol produced from retinal by retinal reductase is then esterified by lecithin-retinol acyltransferase and incorporated into the lipid core of the chylomicron (12). The retinyl esters associated with chylomicrons are cleared into hepatocytes when they undergo a cycle of hydrolysis and re-esterification before storage (12).

It is generally believed that retinol secreted from the liver bound to plasma retinol-binding protein serves as the major source of retinoids for peripheral tissues (8). However, there is growing evidence that a number of cell types are capable of utilizing β-carotene directly, supplementing their own retinoid stores even though serum levels of retinol are tightly controlled. For instance, in addition to the small intestine, β-carotene is converted to retinol in the liver (8), human colon cancer cells (13), and human lung (14) and skin fibroblasts (15).

Significant progress in understanding the tissue-specific uptake and metabolism of β-carotene was provided through the molecular characterization of β,β-carotene 15,15′-dioxygenases from the fruit fly (16), chicken (17), mouse (18, 19), and human (20). Northern blot analysis of the corresponding mRNAs revealed that besides the small intestine, many tissues, including liver, kidney, brain, stomach, testis, and small intestine express relatively high levels of β,β-carotene 15,15′-dioxygenase (17–20). *In situ* hybridization analysis of β-carotene dioxygenase expression showed that the corresponding mRNA was expressed primarily in epithelial structures of tissues such as duodenum, lung, and kidney as well as in skin, where it could serve to provide the tissue-specific vitamin A supply (21). Re-

* This work was supported by the National Institute on Alcohol Abuse and Alcoholism Grants AA00221 and AA12153 (to N. Y. K.) and by NCI, National Institutes of Health Grant CA75173 and Department of Defense Grant PC991274 (to P. S. N.). The costs of publication of this article were defrayed in part by the payment of page charges. This article must therefore be hereby marked "*advertisement*" in accordance with 18 U.S.C. Section 1734 solely to indicate this fact.

§ To whom correspondence should be addressed: Division of Molecular Biology and Biochemistry, School of Biological Sciences, University of Missouri-Kansas City, 5007 Rockhill Rd., 103 BSB, Kansas City, MO 64110. Tel.: 816-235-2658; Fax: 816-235-5595; E-mail: kedishvilin@umkc.edu.

¶ Present address: Dept. of Biochemistry and Molecular Biology, The University of Kansas Medical Center, 3901 Rainbow Blvd., Kansas City, KS 66160-7421.

[1] The abbreviations used are: CRBPII, cellular retinol binding protein type II; SDR, short-chain dehydrogenase/reductase; mAb, monoclonal antibody; BSA, bovine serum albumin; CMV, cytomegalovirus; PBS, phosphate-buffered saline; Endo H, endoglycosidase H; HPLC, high performance liquid chromatography; ER, endoplasmic reticulum.

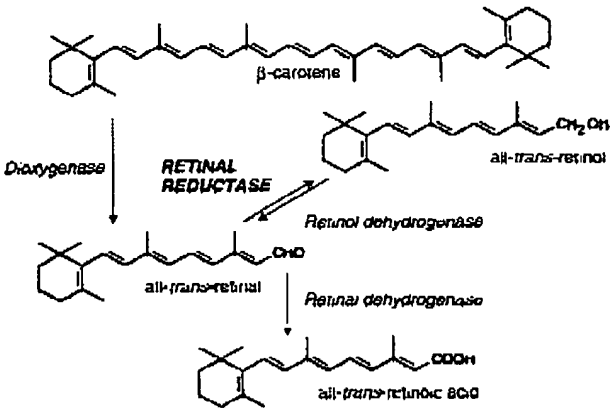

FIG. 1. **Biosynthesis of retinoic acid from β-carotene.**

cently, prostate epithelial cell lines LNCaP, PC-3, and DU 145 were shown to convert β-carotene to retinol (22), suggesting that human prostate epithelium also contains β-carotene dioxygenase. However, the one or more enzymes responsible for the reduction of retinal produced from β-carotene to retinol in prostate as well as other tissues have yet to be characterized. Furthermore, the enzyme responsible for the intestinal microsomal retinal reductase activity that recognizes CRBP II-bound retinal as substrate has not yet been defined at the molecular level.

Recently, we have shown that the prostate expresses high levels of a transcript encoding a novel member of the short-chain dehydrogenase/reductase (SDR) superfamily, *PSDR1* (23). In the present study we characterized the cell-specific expression, subcellular localization, and catalytic properties of the protein encoded by the human *PSDR1* gene. We present evidence that PSDR1 is a microsomal retinal reductase that is expressed in the epithelial cells of the human prostate gland and is capable of reducing all-*trans*-retinal to all-*trans*-retinol under physiologically relevant conditions. This activity suggests that PSDR1 might contribute to the enzymatic conversion of retinaldehyde produced from β-carotene to retinol in human prostate. To provide a nomenclature more descriptive of actual biochemical activity, we have changed the designation of this gene and encoded protein from *PSDR1* to *RalR1* for Retinal Reductase 1.

EXPERIMENTAL PROCEDURES

RalR1 Monoclonal Antibody—A peptide located near the C terminus of RalR1, CH$_3$CO-CHVAWVSVRARNETIAR-CONH$_2$ (residues 287–303), was synthesized (Genemed Synthesis, Inc., South San Francisco, CA) and conjugated to maleimide-activated keyhole limpet hemocyanin (Pierce, Rockford, IL) through the N-terminal Cys of the peptide. Mice were immunized with the keyhole limpet hemocyanin-peptide conjugate, and a monoclonal antibody (mAb) was generated in the Biologics Production Facility of the Fred Hutchinson Cancer Research Center. Hybridomas were screened by enzyme-linked immunosorbent assay using bovine serum albumin (BSA) conjugated with the RalR1 peptide as a positive control and BSA conjugated with unrelated peptides as negative controls. Positive clones were further screened by immunoblotting using COS-7 cells transfected with RalR1 expression vectors. One hybridoma clone producing RalR1-specific mAb, designated H8, was used throughout this study.

Immunostaining of Human Prostate—Six-micron sections of formalin-fixed, paraffin-embedded blocks of prostate tissue were deparaffinized and rehydrated in sequential solutions of xylene and ethanol. The sections were sequentially immersed in a 3% aqueous solution of hydrogen peroxide to inactivate endogenous peroxidase activity, a 1% solution of bovine serum albumin in phosphate-buffered saline to block nonspecific protein binding, and then microwaved for 15 min in a 10 mM citrate buffer to "unmask" antigenicity. The sections were immunostained using a three-step indirect avidin-biotin-peroxidase method. The primary antibody was mouse monoclonal anti-RalR1, which was affinity-purified on a protein G column. The negative controls for antibody specificity consisted of non-immune mouse serum and preincubation of the anti-RalR1 antibody with 10-fold molar excess of RalR1 peptide for 2 h before subsequently incubating the monoclonal antibody/peptide solution with tissue sections. Immunoreactivity of the primary antibody was detected using an avidin-biotin-peroxidase kit (Dako Corp., Carpinteria, CA). The diaminobenzidine reaction product was enhanced with an 8% aqueous solution of nickel chloride, which yields a black reaction product. The sections were counterstained with a methyl green nuclear stain prior to coverslipping.

RalR1 Subcellular Localization—A chimeric RalR1-FLAG-tagged protein was constructed by amplifying the full-length RalR1 coding sequence by one PCR using primers PSDR1–5 (5′-TTAAGCTTGCGGC-CGCGAATTCCACC-3′) and PSDR1–3 (5′-TCACTATCTAGAGTC-TATTGGGACCCCACCAG-3′). The product was sequence-verified, cleaved with *Not*I and *Xba*I enzymes, and cloned into the p3XFLAG-CMV-14 expression vector (Sigma-Aldrich, St. Louis, MO). COS-7 monkey kidney cells (American Type Culture Collection, Manassas, VA) were grown on eight-well culture slides and transiently transfected with RalR1-FLAG using FuGENE 6 transfection reagent according to a protocol supplied by the manufacturer (Roche Molecular Biochemicals, Indianapolis, IN). Twenty-four hours after transfection, cells were washed with PBS and then fixed with 30% acetone/70% methanol mixture for 10 min at −20 °C. The cells were soaked in 3% BSA/PBS for 1 h for blocking. The primary antibody, either anti-RalR1 or M2 anti-FLAG (Sigma), was added at 1–3 μg/ml and incubated for 1 h at room temperature. The cells were washed five times with PBS containing 0.1% Tween-20 and incubated with anti-mouse IgG-conjugated with biotin (Pierce) for 30 min, followed by incubation with streptavidin-fluorescein isothiocyanate conjugate (Pierce). The cells were washed five times with PBS plus 0.1% Tween-20 between the incubations. The same immunostaining procedure was followed using the anti-RalR1 antibody on LNCaP cells grown using growth conditions suggested by the supplier (American Type Culture Collection). Mounting medium (Vector Laboratories, Inc., Burlingame, CA) was applied to each well, and the slides were immediately examined using a fluorescence microscope (Olympus) equipped with a wide-field deconvolution system (DeltaVision, Applied Precision Incorporated, Issaquah, WA). Typically, 30 images were collected per section with a plane width of 0.3 μm per image through the cell center.

Expression in Sf9 Cells—The coding region of the cDNA for human RalR1 was cloned into *Eco*RI restriction site of pVL1393 Baculovirus transfer vector. The *RalR1*-pVL1393 construct with the correct orientation of the insert was selected based on restriction endonuclease digest analysis and was confirmed by DNA sequencing. Cotransfection of Sf9 cells with the transfer vector and linearized BaculoGold DNA was performed according to the manufacturer's protocol (BD PharMingen, San Diego, CA). The recombinant virus was amplified and used to produce RalR1 protein essentially as described previously for human RoDH-4 (24). The subcellular fractions were isolated by sequential centrifugations of the cell homogenate prepared using French press. The unbroken cells, cellular debris, and nuclei were removed by centrifugation at 1,000 × *g* for 10 min. Mitochondria were pelleted by centrifugation at 10,000 × *g* for 30 min, and microsomal fraction was isolated by centrifugation at 105,000 × *g* for 1 h through a 0.6 M sucrose cushion. Microsomes were resuspended in 0.1 M potassium phosphate, pH 7.4, 0.1 mM EDTA, 1 mM dithiothreitol, 20% glycerol, aliquoted, and stored frozen at −70 °C. Protein concentration was determined by Lowry *et al.* (25) using bovine serum albumin as a standard.

Western Blot Analysis, Endoglycosidase H Treatment, and Coupled in Vitro Transcription/Translation—Western blot analysis of RalR1 expression was performed using a 1:100 dilution of RalR1 mAb. Protein was detected using ECL Western blotting analysis system (Amersham Biosciences, Piscataway, NJ) as described previously (26). For endoglycosidase H (Endo H) treatment, 20 μg of microsomal protein was resuspended in 50 mM sodium phosphate buffer, pH 5.5, containing 0.1% SDS, and 0.1 M 2-mercaptoethanol. The protease inhibitor phenylmethylsulfonyl fluoride was added to a 5 mM final concentration. One half of the mixture was treated with 2.5 μl (12.5 units) of Endo H (Roche Molecular Biochemicals), and the other half received 2.5 μl of the buffer. Both samples were incubated overnight at room temperature, then denatured with SDS-PAGE loading buffer for 5 min at 94 °C and analyzed by Western blotting. 11β-Hydroxysteroid dehydrogenase type 1 with the FLAG epitope MDYKDDDD-COOH (Sigma) attached to the C terminus served as a positive control for glycosylation in Sf9 cells and deglycosylation by Endo H.

For *in vitro* protein synthesis, RalR1 cDNA cloned into pCR2.1-

TOPO vector (Invitrogen) was subjected to transcription by T7 RNA polymerase and translation in reticulocyte lysate in the presence or absence of dog pancreas microsomes (TNT Quick system, Promega, Madison, WI) according to the manufacturer's instructions. In a typical assay, 0.5–1 μg of plasmid DNA, 20 μCi of [^{35}S]methionine (Amersham Biosciences) and 0.5–1 μl of canine pancreatic microsomal membranes (Promega) were incubated for 60–90 min at 30 °C in a final volume of 12.5 μl. ^{35}S-Labeled proteins were subjected to 12% SDS-PAGE and analyzed by autoradiography.

Analysis of Enzymatic Activity—Catalytic activity of RalR1 was assayed in 90 mM potassium phosphate, pH 7.4, and 40 mM KCl at 37 °C (reaction buffer) in siliconized glass tubes as described previously (24). The oxidative and reductive activity of RalR1 toward retinoid substrates was analyzed using all-*trans* and *cis* isomers of retinoids (Sigma-Aldrich). The stock solutions of retinoid substrates were prepared in ethanol, and their concentrations were determined based on the corresponding extinction coefficients at the appropriate wavelengths. Ethanol-dissolved retinoids were solubilized in the reaction buffer by a 10-min sonication in the presence of equimolar delipidated bovine serum albumin. The concentration of ethanol in the reaction mixture did not exceed 0.3%. At this concentration, ethanol had no effect on RalR1 activity. The 500-μl reactions were started by the addition of cofactor and carried out for 15–30 min at 37 °C. The amount of protein in the reaction mixture varied from 1 to 250 μg. The reactions were terminated by the addition of an equal volume of cold ethanol supplemented with 100 μg/ml butylated hydroxytoluene. Retinoids were extracted using solid-phase extraction on a Waters Sep-Pak C18 (light) column as described before (27) and analyzed using a Waters Alliance HPLC system. Elution was monitored at 350 nm with a Waters 2487 Dual Absorbance Detector. Unless stated otherwise, retinoids were separated using normal-phase HPLC. The stationary phase was Waters Spherisorb S3W column (4.6 mm × 100 mm), and the mobile phase consisted of hexane:acetone (90:10, v/v). The flow rate was 1 ml/min. Under these conditions, all-*trans*-retinaldehyde and all-*trans*-retinol eluted at 2.09 and 4.095 min, respectively. The peak detection limits were ~1.0 pmol for all-*trans*-retinal and ~2.5 pmol for all-*trans*-retinol. The elution times for other isomers were as follows: 3.96 min for 9-*cis*-retinol, 3.28 min for 13-*cis*-retinol, 1.94 min for 9-*cis*-retinaldehyde, and 1.83 min for 13-*cis*-retinaldehyde. Retinoids were quantitated by comparing their peak areas to a calibration curve constructed from the peak areas of a series of standards.

The oxidative and reductive activity of RalR1 toward steroids was analyzed using tritiated steroids (PerkinElmer Life Sciences, Boston, MA, ~40–60 Ci/mmol each), which were diluted with cold steroids (Steraloids Inc., Newport, RI, and Sigma-Aldrich) dissolved in Me_2SO (<1% in the reaction mix) (24, 26, 27). Dihydrotestosterone (5α-androstan-17β-ol-3-one), progesterone (4-pregnen-3,20-dione), corticosterone (4-pregnen-11β,21-diol-3,20-dione), aldosterone (4-pregnen-11β,21-diol-3,18,20-trione), androsterone (5α-androstan-3α-ol-17-one), dehydroepiandrosterone (5-androsten-3β-ol-17-one), allopregnanolone (5α-pregnan-3α-ol-20-one), and 3α-androstanediol (5α-androstan-3α,17β-diol) were tested as substrates either in the oxidative direction in the presence of 1 mM $NADP^+/NAD^+$ or in the reductive direction in the presence of 1 mM NADPH/NADH. The amount of microsomal protein in the reaction mixture varied from 25 to 250 μg. Control reactions contained the same amount of microsomal protein isolated from Sf9 cells that were infected with wild-type virus. The 250-μl reactions were started with the addition of cofactor and incubated at 37 °C for 15–120 min. The reaction products were extracted and separated by development in chloroform:ethyl acetate (3:1, v/v) on silica gel TLC plates. After drying, TLC plates were exposed to a PhosphorImager tritium screen and analyzed using a PhosphorImager (Amersham Biosciences).

Determination of Kinetic Constants—Steady-state kinetic analysis was performed in 90 mM potassium phosphate, pH 7.4, and 40 mM KCl at 37 °C as described above. The reaction rate was linearly proportional to the amount of microsomes added per 500-μl reaction volume with up to 2 μg of protein in the reductive direction and with up to at least 10 μg of protein in the oxidative direction during the 15-min incubation time. Kinetic analysis of substrates in the reductive direction was performed with 0.625 μg of protein and in the oxidative direction with 7.5 μg per 500-μl reaction volume, so that the amount of product formed after 15 min of incubation did not exceed 10% of the initial substrate amount. Under these conditions, the background level of product formed by microsomes from Sf9 cells infected with wild-type virus did not exceed the "minus cofactor" value obtained with the same amount of enzyme-containing microsomes. A control without added cofactor was included for each concentration of substrate and was subtracted from each experimental data point. The amount of product formed in the presence of cofactor was at least 3-fold higher than that in the "minus cofactor" control. The apparent K_m values for oxidation and reduction of retinoids were determined at a fixed $NADP^+$ (1 mM) or NADPH (0.5 mM) concentrations. Each K_m determination was repeated at least three times using six concentrations of each substrate: all-*trans*-retinal (0.25–2.5 μM), 13-*cis*-retinal (0.2–2.5 μM), 9-*cis*-retinal (0.062–2.5 μM), and all-*trans*-retinol (0.5–10 μM). The values of initial velocities (nmol/min of product formed per mg of protein) were obtained by non-linear regression analysis. The apparent K_m values for cofactors were determined at a fixed saturating concentration of all-*trans*-retinal or all-*trans*-retinol with five concentrations of each cofactor. NADPH (0.125–25 μM), NADH (0.0625–2.0 mM), $NADP^+$ (1.25–15 μM), and NAD^+ (0.25–5 mM).

CRBPI was expressed in *Escherichia coli* as a fusion protein with glutathione *S*-transferase and purified using glutathione agarose column as described previously (28). The purified fusion protein was cleaved with thrombin and separated from glutathione *S*-transferase on a Q-Sepharose column by elution with a 0 to 500 mM NaCl gradient in 10 mM Tris, pH 7.4. The amount of functional protein was determined from the fluorescence titration curve of apo-CRBPI with retinol (29). Typically, over 90% of purified CRBPI preparation was capable of binding all-*trans*-retinol (24, 28).

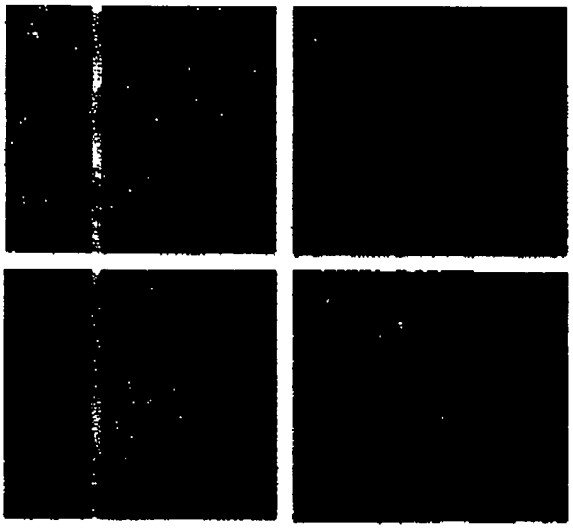

FIG. 2. **Cellular and subcellular distribution of RalR1 protein.** *A*, representative section demonstrating the expression of endogenous RalR1 protein in normal prostate tissue. High immunoreactivity is apparent in the luminal and basal epithelial cells (*black* reaction product). Stromal fibroblast and smooth muscle cell immunoreactivity was not observed. *B*, expression of endogenous RalR1 protein in the LNCaP prostate cancer cell line. Microscopic image of COS-7 cells transfected with RalR1-3 LAG fusion construct and processed for FLAG (*C*) or RalR1 (*D*) immunoreactivity. The pattern of RalR1 expression localizes to the endoplasmic reticulum.

RESULTS

Expression of RalR1 in Prostate Epithelium—We have previously shown that transcripts encoding RalR1 were most highly expressed in the normal prostate gland relative to all other human tissues (23). To localize the one or more specific prostate cell types expressing RalR1, we immunostained normal prostate tissue with anti-RalR1 monoclonal antibodies. High levels of RalR1 protein expression were detected in luminal epithelial cells (Fig. 2*A*). Staining was also present in basal epithelium with undetectable staining in the smooth muscle and fibroblast components of the prostate stroma. This result indicated that the novel SDR protein, RalR1, was specifically expressed in the epithelial cells of human prostate.

Subcellular Localization of RalR1 in Eukaryotic Cells—The retinal reductase activity described previously in the rat small intestine was associated with the microsomal membranes (10).

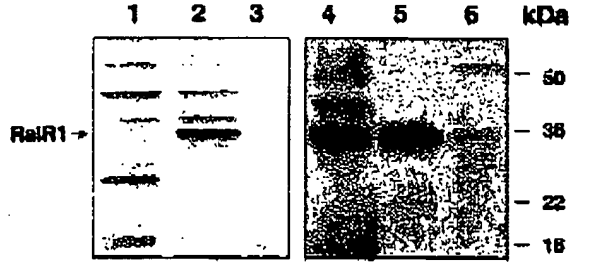

FIG. 3. **Characterization of RalR1 protein.** *Lanes 1–3*, SDS-PAGE analysis of the expressed protein in Sf9 microsomes: *lane 1*, wild-type Sf9 microsomes (10 μg), *lane 2*, Sf9 microsomes containing RalR1 (10 μg); *lane 3*, SeeBlue Plus2 pre-stained protein molecular weight standards (invitrogen) *Lane 4*, ^{35}S-labeled RalR1 synthesized *in vitro* using coupled transcription/translation system (1.25 μl of reaction) *Lanes 5* and *6*, Western blot analysis of RalR1-containing Sf9 microsomes (*lane 5*, 10 μg) and wild-type virus infected Sf9 microsomes (*lane 6*, 10 μg). Antibodies were used at a 1:100 dilution.

To determine the subcellular localization of RalR1, we immunostained the human prostate carcinoma cell line LNCaP with anti-RalR1 antibody (Fig. 2*B*). The immunofluorescent signals (*green*) were localized to the endoplasmic reticulum (ER), indicating that RalR1 was expressed and retained in the ER. RalR1 expression in LNCaP cells was higher than in PC3 prostate carcinoma cells (data not shown), a cell type that we have previously shown expresses low levels of RalR1 message (23). To obtain further evidence for the association of RalR1 with the ER membranes, we determined whether a recombinant RalR1 was also targeted to the ER in non-prostate cell line. COS-7 cells were transfected with a construct expressing the recombinant RalR1 polypeptide fused to a 3×-FLAG tag and immunostained with the M2 anti-FLAG antibody. RalR1 expression again localized to the ER of COS-7 cells (Fig. 2*C*). To confirm this finding, COS cells transfected with RalR1 were immunostained with anti-RalR1 mAb (Fig. 2*D*). The pattern of immunofluorescence was indistinguishable from the pattern observed with the anti-FLAG antibody. These results indicated that RalR1 polypeptide contained the ER targeting signal and appeared to be associated with the ER membranes, similar to the rat intestinal retinal reductase.

Expression of the Human RalR1 Protein in Sf9 Cells—The next objective was to determine whether RalR1 was active toward retinoid substrates. We expressed the full-length cDNA for RalR1 in insect Sf9 cells using the BaculoGuld Baculovirus system. Sf9 cells were homogenized and fractionated into mitochondria, microsomes, and cytosol. The subcellular localization of the recombinant protein in Sf9 cells was determined by Western blot analysis using monoclonal antibodies against RalR1. The majority of the immunoreactive protein was associated with the microsomal fraction (Fig. 3, *lanes 2* and *5*), indicating that RalR1 was targeted to the ER. At the same time, control microsomes isolated from Sf9 cells infected with wild-type virus were not stained with anti-RalR1 mAbs (Fig. 3, *lane 6*).

Because RalR1 localized to the microsomes, we investigated whether it was exposed to the lumenal side of the membrane by examining its glycosylation state. The RalR1 polypeptide contains two *N*-linked glycosylation motifs at Asn^{174} (^{174}NVS^{176}) and Asn^{296} (^{296}NET^{300}). Glycosylated proteins can be detected by their slower electrophoretic mobility relative to that of the non-glycosylated forms. Treatment of microsomal RalR1 expressed in Sf9 cells with Endo H did not change the mobility of the protein (data not shown), indicating that RalR1 was not glycosylated. A control protein, 11β-hydroxysteroid dehydrogenase type 1, was efficiently deglycosylated by Endo H. To obtain further evidence for the lack of RalR1 glycosylation, we compared the electrophoretic mobility of ^{35}S-labeled RalR1 produced *in vitro* using a coupled transcription/translation system in the absence of microsomes (Fig. 3, *lane 4*) to that of the recombinant RalR1 expressed in Sf9 cell microsomes (Fig. 3, *lane 5*). Both samples were separated in the same gel and transferred to a nitrocellulose filter, which was then cut in half. The filter containing ^{35}S-labeled RalR1 was exposed to x-ray film, whereas the second filter was hybridized with anti-RalR1 mAbs to visualize the microsomal RalR1 by chemiluminescence. Alignment of the two images revealed that the microsomal RalR1 had electrophoretic mobility identical to that of RalR1 produced in the absence of microsomes (Fig. 3). To confirm this result, we compared the electrophoretic mobility of ^{35}S-labeled RalR1 preparations synthesized *in vitro* in the absence and presence of canine microsomal membranes. Canine microsomes efficiently glycosylated yeast α-mating factor, which was provided with the kit (data not shown), but RalR1 was not glycosylated. Because glycosylation occurs exclusively in the lumen of the ER, these results suggested that the segment of RalR1 containing the putative glycosylation motifs was not exposed to the ER lumen.

Analysis of RalR1 Substrate and Cofactor Specificity—Experiments were designed to compare the retinoid-metabolizing activity of Sf9 cells expressing RalR1 with the activity of Sf9 cells infected with wild-type virus. Homogenates of RalR1-Sf9 and virus-Sf9 cells were incubated with 1 μM all-*trans*-retinol or 1 μM all-*trans*-retinal in the presence of the oxidative ($NAD^+/NADP^+$) or reductive (NADH/NADPH) cofactors, respectively. The reaction products were extracted and analyzed by reverse-phase HPLC. In the oxidative direction, a maximum of only about 10% of substrate conversion was observed over a wide range of protein concentrations (up to 250 μg) (data not shown). However, when RalR1 was analyzed in the reductive direction, more than 90% of all-*trans*-retinal was converted to all-*trans*-retinol in the presence of NADPH (Fig. 4*A*). The same amount (micrograms) of homogenate obtained from control cells infected with wild-type virus produced at least 10-fold less all-*trans*-retinol (Fig. 4*B*). This result indicated that the observed retinal reductase activity was associated with RalR1. Percent conversion was generally lower in the presence of NADH for both RalR1- and wild-type virus infected cells (Fig. 4, *C* and *D*).

To determine whether retinal reductase activity colocalized with RalR1 protein in the microsomal fraction of the homogenate, we determined the activity of the subcellular fractions isolated from RalR1-expressing Sf9 cells. Similar to RalR1 protein distribution, over 90% of the retinal reductase was recovered with the microsomes (data not shown). No activity was detected in the microsomal fraction of Sf9 cells infected with wild-type virus, indicating that the low background activity observed with Sf9 cell homogenate in the presence of $NADP^+$ (Fig. 4) was due to the cytosolic enzymes. As determined by normal-phase HPLC analysis, the major product of all-*trans*-retinal reduction catalyzed by microsomal RalR1 was all-*trans*-retinol, although small amounts of 13-*cis* isomers of retinol and retinal were recovered as well (Fig. 5*A*). Isomerization of retinoids during extraction procedures was also observed by other investigators (10, 30). Therefore, the reaction products were quantified by summing the areas of both peaks.

The next question was whether RalR1 exhibited specificity for all-*trans*-retinal or whether it was also active toward *cis*-retinals. Kinetic analysis of the same preparation of microsomal RalR1 revealed that the enzyme recognized 9-*cis*-retinal and 13-*cis*-retinal as substrates with affinity similar to that for all-*trans*-retinal (K_m values of 0.19–0.62 μM) (Table I). How-

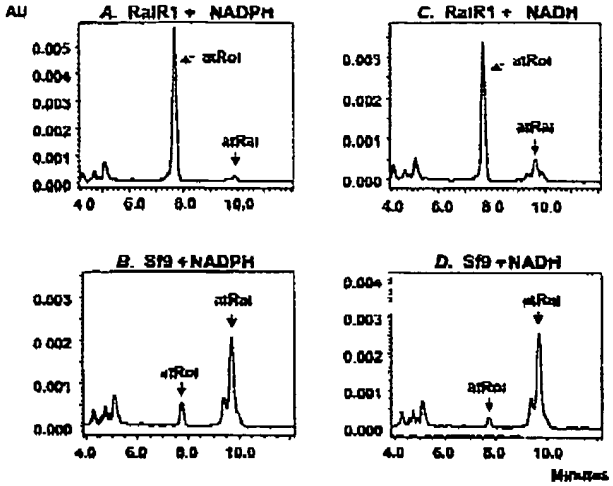

FIG 4. **Reverse-phase HPLC analysis of the reductive activity of RalR1 toward all-*trans*-retinal.** Homogenates (250 μg per reaction) of Sf9 cells infected with RalR1 (*A* and *C*) or wild-type baculovirus (*B* and *D*) were incubated with 1 μM all-*trans*-retinal in the presence of 1 mM NADPH (*A* and *B*) or 1 mM NADH (*C* and *D*) for 30 min at 37 °C. The reactions were terminated by the addition of an equal volume of cold ethanol supplemented with 100 μg/ml butylated hydroxytoluene. Retinoids were extracted using solid-phase extraction on a Waters Sep-Pak C18 column as described before (27) and reconstituted into 200 μl of mobile phase acetonitrile-water-ammonium acetate (87.5:2.5:10.0, v/v). Ten-microliter aliquots were analyzed by reverse-phase HPLC using a 3.5-μm Waters Symmetry column (4.6 × 150 mm). The flow rate was 1 ml/min. Under these conditions, all-*trans*-retinol and all-*trans*-retinaldehyde eluted at 7.7 and 9.5 min, respectively.

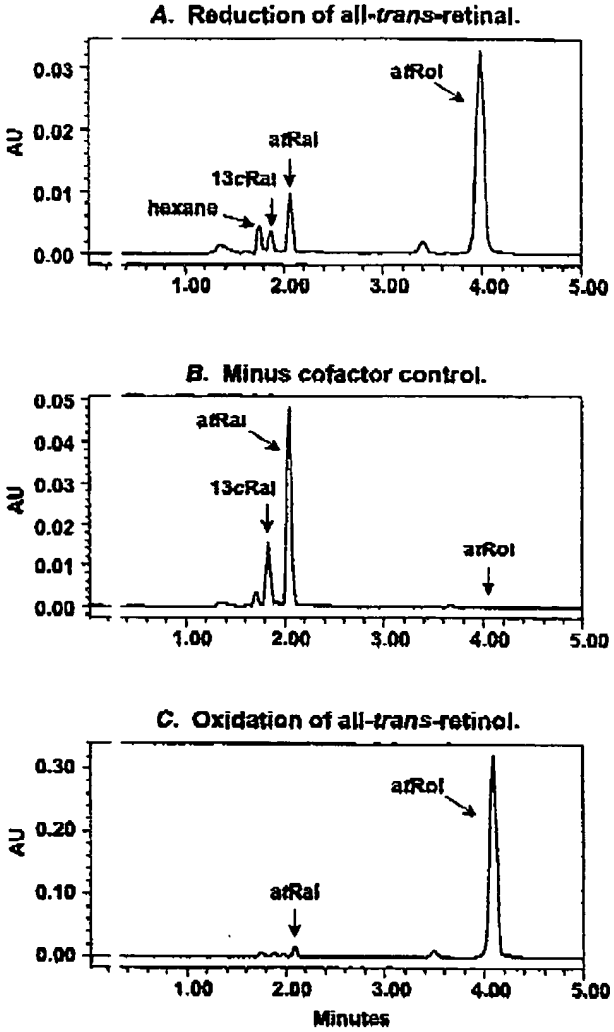

FIG. 5. **Normal-phase HPLC chromatogram of retinoids produced by RalR1 in the reductive and oxidative direction.** *A*, reduction of 1.25 μM all-*trans*-retinal to all-*trans*-retinol catalyzed by 10 μg of RalR1 containing Sf9 microsomes in the presence of 1 mM NADPH. All *trans*-retinal partially isomerized into 13-*cis*-retinal during manipulations. *B*, the "minus cofactor control" for the reductive direction. *C*, oxidation of 10 μM all-*trans*-retinol to all-*trans*-retinal catalyzed by 1.5 μg of RalR1-containing Sf9 microsomes in the presence of 1 mM NAD^+.

ever, the reaction rate with *cis*-retinals was severalfold lower than with all-*trans*-retinal (Table I). Thus, RalR1 was most efficient as an all-*trans*-retinal reductase. In addition, the utilization ratio of RalR1 in the reductive direction was about 50-fold higher than in the oxidative direction with all-*trans*-retinol as substrate (Table I and Fig. 5*C*). The preference of RalR1 for the reductive direction was consistent with the apparent K_m values for cofactors. The enzyme exhibited a ~3000-fold lower K_m value for NADPH, the predominant reductive cofactor in the cells, than for NAD^+, the major oxidative cofactor (Table II).

Having established that RalR1 was most efficient as an all-*trans*-retinal reductase, we determined if RalR1 could function in the presence of cellular retinol binding protein, which was previously shown to completely sequester retinol and retinal from nonspecific enzymes (10, 28, 31). It was suggested that the microsomal retinal reductase activity previously described in the rat small intestine was important for retinoid metabolism, because, in contrast to the retinal reductase activity present in the cytosol, the microsomal activity reduced retinal in the presence of a 20% molar excess of CRBPII (10). The expression of CRBPII is restricted to the small intestine. Other tissues, including the prostate (32, 33), contain a different binding protein, CRBP type I, which binds all-*trans*-retinal and all-*trans*-retinol with even higher affinity than CRBPII (K_d values of 50 and <10 nM, respectively, compared with ~100 nM for CRBPII) (reviewed in Ref. 34). To determine whether RalR1 was capable of reducing all-*trans*-retinal in the presence of CRBPI, we titrated the reaction mixture with an increasing amount of the binding protein. As can be seen in Fig. 6, the addition of a 2.5-fold excess of CRBPI to the reaction mixture resulted in a decrease of ~6.5-fold in the rate of retinal reduction, from 8.5 nmol/min × mg at 1 μM all-*trans*-retinal down to 1.3 nmol/min × mg. However, further increases in the amount of added CRBPI had little effect on RalR1 activity. The reaction rate remained constant with up to a 10-fold molar excess of CRBPI relative to the retinal concentration (Fig. 6). This result indicated that RalR1 reduced retinal in the presence of a wide range of CRBPI concentrations.

Because several retinoid-metabolizing members of the SDR superfamily were shown to recognize 3α- and 17β-hydroxy and ketosteroid as substrates (24, 27, 35, 36), we tested whether RalR1 was also active toward steroids. Steroid compounds were used at a 2 μM concentration in the presence of either 1 mM NAD^+/$NAD(P)^+$ or 1 mM NADH/NADPH. The reaction products were extracted and analyzed by TLC using a PhosphorImager. The oxidative retinol/sterol dehydrogenases characterized previously in our laboratory (24, 27) served as positive controls for steroid oxidoreductase activity. RalR1 did not possess any significant activity toward oxidation or reduction of the functional

TABLE I
Kinetic constants for retinoid substrates

Kinetic constants for the reduction of retinals were determined in the presence of saturating NADPH (0.5 mM). Kinetic constants for the oxidation of all-*trans*-retinol were determined at saturating $NADP^+$ (1 mM) (*Experimental Procedures*). Kinetic constants shown in this table were determined using the same preparation of microsomes containing RalR1 and were calculated using GraFit (Erithacus Software Ltd.) and expressed as the means ± S.D. Similar constants were obtained using three independent preparations of microsomal RalR1.

Substrate	Apparent K_m	Apparent V_{max}	V_{max}/K_m
	μM	nmol/(min × mg microsomal protein)	
All-*trans*-retinal	0.50 ± 0.05	18.0 ± 0.5	36
13-*cis*-retinal	0.62 ± 0.05	7.0 ± 0.3	11
9-*cis*-retinal	0.19 ± 0.04	1.6 ± 0.1	8.4
All-*trans*-retinol	1.3 ± 0.2	0.95 ± 0.04	0.7

TABLE II
Apparent K_m values for cofactors

The apparent K_m values for NADPH and NADH were determined with saturating all-*trans*-retinal (5 μM). The apparent K_m values for $NADP^+$ and NAD^+ were determined with saturating all-*trans*-retinol (15 μM) ("Experimental Procedures")

Cofactor	K_m
	μM
NADPH	0.23 ± 0.02
NADH	1300 ± 200
$NADP^+$	0.8 ± 0.2
NAD^+	680 ± 80

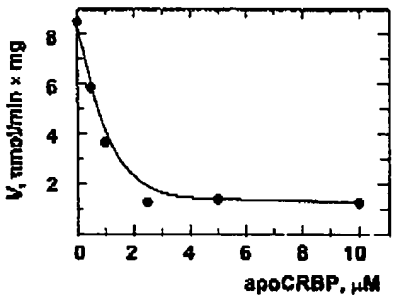

FIG. 6. **Analysis of RalR1 activity toward all-*trans*-retinal in the presence of CRBPI.** All-*trans*-retinal was used at a concentration of 1 μM. CRBPI concentration varied from 0.5 to 10 μM. The amount of microsomes in each 0.5-ml reaction was 2 μg. The result shown is representative of at least three independent experiments.

hydroxyl or ketone groups in positions 3, 17, or 20, relative to the background activity of Sf9 cells infected with wild-type virus (data not shown). Thus, RalR1 appeared to be specific for retinoids and was most efficient as an NADPH-dependent retinal reductase.

DISCUSSION

In the present study we have established that the protein encoded by the recently discovered human gene originally named *PSDR1* for prostate short-chain dehydrogenase/reductase encodes a novel microsomal enzyme with retinal reductase activity. Accordingly, we changed the designation of *PSDR1* gene and protein to *RalR1* for retinal reductase 1. RalR1 shares less than 30% overall sequence identity with other members of the SDR superfamily, including the recently characterized all-*trans*-retinal reductase retinal SDR1 (37) and the $NADP^+$-dependent photoreceptor-specific all-*trans*-retinol dehydrogenase photoreceptor retinol dehydrogenase (38). Analysis of the primary structure of RalR1 based on algorithms for secondary structure prediction (39, 40) suggests that RalR1 is a membrane protein anchored by a single hydrophobic N-terminal segment (amino acids 1–23) with the majority of the polypeptide chain localized on the cytosolic side of the membrane. This model is supported by the experimental data obtained in the present study. First of all, as established by cell fractionation and immunolocalization studies, RalR1 is associated with the ER membranes. Second, the subunit molecular weight of RalR1 does not change after incubation with microsomes, indicating that the ER targeting signal in RalR1 is not cleaved. Finally, RalR1 is not glycosylated at the putative *N*-linked glycosylation motifs at Asn^{174} and Asn^{268}. Because glycosylation occurs exclusively in the lumen of the ER, lack of glycosylation suggests that RalR1 faces the cytosolic side of the ER membrane.

The cytosolic orientation of RalR1 in the ER membrane suggests that in intact cells the enzyme will function as a reductase. RalR1 exhibits at least an 800-fold lower K_m values for $NADP^+$ and NADPH than for NAD^+ and NADH as cofactors. In the cytosol of liver and, presumably, other cells, $NADP^+$ exists mainly in the reduced form (41). Therefore, enzymes that prefer $NADP^+$ are likely to function in the reductive direction *in vivo*.

Characterization of RalR1 enzymatic properties revealed that the enzyme recognizes retinoids but not steroids as substrates and is particularly efficient as an all-*trans*-retinaldehyde reductase. Retinoids are highly hydrophobic and chemically labile compounds that are solubilized and protected from unwanted conversions by specific binding proteins inside the cells and in blood plasma (reviewed in Ref. 34). All-*trans*-retinal binds to cytosolic CRBPI, which is expressed in many different types of cells but the levels of CRBPI expression may vary (32). Most likely, the enzymes involved in retinoid metabolism have to function in the presence of some amount of CRBPI. Interestingly, not all enzymes that are active with free retinol can metabolize retinol in the presence of CRBPI. It was shown that CRBPI sequesters all-*trans*-retinol from acyl CoA:retinol acyltransferase (29, 31, 42, 43) and from human cytosolic alcohol dehydrogenase class IV (28), enzymes that are active with free retinol. On the other hand, retinal reductase activity in the rat intestine reduced all-*trans*-retinal in the presence of a 20% molar excess of CRBPII (10) and the cytosolic rat retinal dehydrogenase type 2 oxidized retinal in the presence of a 2-fold molar excess of CRBPI (3).

The ratio of CRBPI to retinaldehyde in the human prostate gland is not known. Kato *et al.* (32) reported that rat prostate contains an ~8-fold lower amount of CRBP than rat liver (5.2 *versus* 40.0 μg/g of wet weight). This translates into ~0.3 μM CRBP in rat prostate (molecular weight 14,600). The molar ratio of CRBP to retinal might vary, depending on the tissue supply of β-carotene and the rate of retinol oxidation to retinaldehyde. Therefore, we investigated the effect of CRBPI on RalR1 activity at a constant concentration of retinal over a wide range of CRBPI concentrations. Our results showed that RalR1 exhibits a relatively high rate (1.3 nmol/min × mg) of retinal reduction even at a 10-fold molar excess of CRBPI over 1 μM retinal concentration. Thus, RalR1 can produce retinol from retinaldehyde in the presence of varied physiological levels of CRBPI.

Retinoic acid plays an important role in the prostate as an activating ligand for retinoic acid receptor γ, which is required

for the normal differentiation of prostate epithelium (44). Accordingly, the prostate gland contains retinol dehydrogenase activity associated with the microsomes and retinal dehydrogenase activity in the cytosol that catalyze the formation of retinoic acid (45). Furthermore, a recent report demonstrated that prostate cells are capable of converting β-carotene to retinol, suggesting that these cells possess β-carotene dioxygenase and retinal reductase activities (22). While our manuscript was under revision, the presence of β-carotene dioxygenase (β-carotene 15,15′-monooxygenase) mRNA in human prostate was directly demonstrated in a study by Lindqvist and Andersson (46), providing further support for colocalization of β-carotene dioxygenase and retinal reductase.

Under normal circumstances, the intracellular levels of retinoic acid in tissues are tightly controlled. The molecular mechanisms responsible for this regulation are not yet fully understood but appear to function at several levels of retinoic acid metabolism: biosynthesis, degradation, and storage. Aberrations in retinoid signaling are early events in carcinogenesis, and vitamin A deficiency has been associated with a higher incidence of cancer (reviewed in Ref. 47). It has been demonstrated that the levels of retinoic acid are five to eight times lower in human prostate cancer than in normal prostate cells (45). Supplementation of the diet with β-carotene appears to decrease the risk of developing prostate cancer (48), and it was shown that β-carotene inhibits the growth of prostate cancer cells *in vitro* (22).

From a metabolic point of view, retinal produced from β-carotene in the prostate or any other peripheral tissue may be either oxidized to bioactive retinoic acid by cytosolic aldehyde dehydrogenases or it may be reduced to retinol, which can then be esterified for storage (8). Hence, retinal is positioned at the crossroads of two opposite metabolic processes: activation and inactivation of retinoids. The fate of the cellular retinal would depend on the activities and expression levels of local aldehyde dehydrogenases and retinal reductases that compete for the same all-*trans*-retinal substrate. Therefore, changes in the expression level of RalR1 could perturb retinoid homeostasis and alter the intracellular retinoic acid concentrations, leading to abnormal differentiation of prostate epithelium.

Besides prostate, RalR1 appears to be expressed at lower levels in a number of different human tissues, including the small intestine (23), where it could play a role in retinoid metabolism. Identification and characterization of retinal reductases in human tissues will provide a better understanding of the control mechanisms responsible for the regulation of intracellular retinoic acid concentrations.

Acknowledgments—We thank Larry True for assistance with immunohistochemistry, and we thank Robert Vessella and the Department of Urology at the University of Washington for providing prostate tissues. We are grateful to Dr. Kirill Popov for a critical reading of the manuscript.

REFERENCES

1. Mangelsdorf, D., Umesono, K., and Evans, R. M. (1994) in *The Retinoids: Biology, Chemistry and Medicine* (Sporn, M. B., Roberts, A. B., and Goodman, D. S., eds) pp. 319–350, Raven Press, New York
2. Zhao, D., McCaffery, P., Ivins, K. J., Neve, R. L., Hogan, P., Chin, W. W., and Drager, U. C. (1996) *Eur. J. Biochem.* 240, 15–22
3. Wang, X., Penzes, P., and Napoli, J. L. (1996) *J. Biol. Chem.* 271, 16288–16293
4. Ambroziak, W., Izaguirre, G., and Pietruszko, R. (1999) *J. Biol. Chem.* 274, 33366–33373
5. Gruen, F., Hirose, Y., Kawauchi, S., Ogura, T., and Umesono, K. (2000) *J. Biol. Chem.* 275, 41210–41218
6. Napoli, J. L. (1999) *Biochim. Biophys. Acta* 1440, 139–162
7. Duester, G. (2000) *Eur. J. Biochem.* 267, 4315–4324
8. Blaner, W. S., and Olson, J. A. (1994) in *The Retinoids: Biology, Chemistry and Medicine* (Sporn, M. B., Roberts, A. B., and Goodman, D. S., eds) pp. 229–256, Raven Press, New York
9. Barua, A. B., and Olson, J. A. (2000) *J. Nutr.* 130, 1996–2001
10. Kakkad, B. P., and Ong, D. E. (1988) *J. Biol. Chem.* 263, 12916–12919
11. Li, E., Demmer, L. A., Sweetser, D. A., Ong, D. E., and Gordon, J. I. (1986) *Proc. Natl. Acad. Sci. U. S. A.* 83, 5779–5783
12. Vogel, S., Gamble, M. V., and Blaner, W. S. (1999) in *Retinoids: The Biochemical and Molecular Basis of Vitamin A and Retinoid Action*, Vol. 139 (Nau, H., and Blaner, W. S., eds.), pp. 31–96, Springer-Verlag, Berlin
13. During, A., Albaugh, G., and Smith, J. C. (1998) *Biochem. Biophys. Res. Commun.* 249, 467–474
14. Scita, G., Aponte, G. W., and Wolf, G. (1992) *J. Nutr. Biochem.* 3, 118–123
15. Wei, R. R., Wamer, W. G., Lambert, L. A., and Kornhauser, A. (1998) *Nutr. Cancer* 30, 53–58
16. von Lintig, J., and Vogt, K. (2000) *J. Biol. Chem.* 275, 11915–11920
17. Wyss, A., Wirtz, G., Woggon, W., Brugger, R., Wyss, M., Friedlein, A., Bachmann, H., and Hunziker, W. (2000) *Biochem. Biophys. Res. Commun.* 271, 334–336
18. Redmond, T. M., Gentleman, S., Duncan, T., Yu, S., Wiggert, B., Gantt, E., and Cunningham, F. X., Jr. (2001) *J. Biol. Chem.* 276, 6560–6565
19. Paik, J., During, A., Harrison, E. H., Mendelsohn, C. L., Lai, K., and Blaner, W. S. (2001) *J. Biol. Chem.* 276, 32160–32168
20. Yan, W., Jang, G. F., Haeseleer, F., Esumi, N., Chang, J., Kerrigan, M., Campochiaro, M., Campochiaro, P., Palczewski, K., and Zack, D. J. (2001) *Genomics* 72, 193–202
21. Wyss, A., Wirtz, G. M., Woggon, W. D., Brugger, R., Wyss, M., Friedlein, A., Riss, G., Bachmann, H., and Hunziker, W. (2001) *Biochem. J.* 354, 521–529
22. Williams, A. W., Boileau, T. W.-M., Zhou, J. R., Clinton, S. K., and Erdman, J. W. (2000) *J. Nutr.* 130, 728–732
23. Lin, B., White, J. T., Ferguson, C., Wang, S., Vessella, R., Bumgarner, R., True, L. D., Hood, L., and Nelson, P. S. (2001) *Cancer Res.* 61, 1611–1618
24. Gough, W. H., VanOoteghem, S., Sint, T., and Kedishvili, N. Y. (1998) *J. Biol. Chem.* 273, 19778–19785
25. Lowry, O. H., Rosebrough, N. H., Farr, A. L., and Randall, R. J. (1951) *J. Biol. Chem.* 193, 265–275
26. Chetyrkin, S. V., Belyaeva, O. V., Gough, W. H., and Kedishvili, N. Y. (2001) *J. Biol. Chem.* 276, 22278–22286
27. Chetyrkin, S. V., Hu, J., Gough, W. H., Dumaual, N., and Kedishvili, N. Y. (2001) *Arch. Biochem. Biophys.* 386, 1–10
28. Kedishvili, N. Y., Gough, W. H., Davis, W. I., Parsons, S., Li, T. K., and Bosron, W. F. (1998) *Biochem. Biophys. Res. Commun.* 249, 191–196
29. Ong, D. E., Kakkad, B., and MacDonald, P. N. (1987) *J. Biol. Chem.* 262, 2729–2736
30. Gamble, M. V., Shang, E., Zott, R. P., Mertz, J. R., Wolgemuth, D. J., and Blaner, W. S. (1999) *J. Lipid Res.* 40, 2279–2292
31. Randolph, R. K., Winkler, K. E., and Ross, A. C. (1991) *Arch. Biochem. Biophys.* 288, 500–508
32. Kato, M., Blaner, W. S., Mertz, J. R., Das, K., Kato, K., and Goodman, D. S. (1985) *J. Biol. Chem.* 260, 4832–4838
33. Pasquali, D., Rossi, V., Prezioso, D., Gentile, V., Colantuoni, V., Lotti, T., Bellastella, A., and Sinisi, A. A. (1999) *J. Clin. Endocrinol. Metab.* 84, 1463–1469
34. Noy, N. (2000) *Biochem. J.* 348, 481–495
35. Biswas, M. G., and Russell, D. W. (1997) *J. Biol. Chem.* 272, 15959–15966
36. Wang, J., Chai, X., Eriksson, U., and Napoli, J. L. (1999) *Biochem. J.* 338, 23–27
37. Haeseleer, F., Huang, J., Lebioda, L., Saari, J. C., and Palczewski, K. (1998) *J. Biol. Chem.* 273, 21790–21799
38. Rattner, A., Smallwood, P. M., and Nathans, J. (2000) *J. Biol. Chem.* 275, 11034–11043
39. von Heijne, G. (1992) *J. Mol. Biol.* 225, 487–494
40. Claros, M. G., and von Heijne, G. (1994) *Comput. Appl. Sci.* 10, 685–686
41. Veech, R. L., Eggleston, L. V., and Krebs, H. A. (1969) *Biochem. J.* 115, 609–619
42. Ong, D. E., MacDonald, P. N., and Gubitosi, A. M. (1988) *J. Biol. Chem.* 263, 5789–5796
43. Yost, R. W., Harrison, E. H., and Ross, A. C. (1988) *J. Biol. Chem.* 263, 18693–18701
44. Lohnes, D., Kastner, P., Dierich, A., Mark, M., LeMeur, M., and Chambon, P. (1993) *Cell* 73, 643–658
45. Pasquali, D., Thaller, C., and Eichele, G. (1996) *J. Clin. Endocrinol. Metab.* 81, 2186–2191
46. Lindqvist, A., and Andersson, S. (2002) *J. Biol. Chem.* 277, 23942–23948
47. Sun, S. Y., and Lotan, R. (2002) *Crit. Rev. Oncol. Hematol.* 41, 41–55
48. Cook, N. R., Stampfer, M. J., Ma, J., Manson, J. E., Sacks, F. M., Buring, J. E., and Hennekens, C. H. (1999) *Cancer* 86, 1783–1792

Tuesday, August 23, 2005 9:16 ,

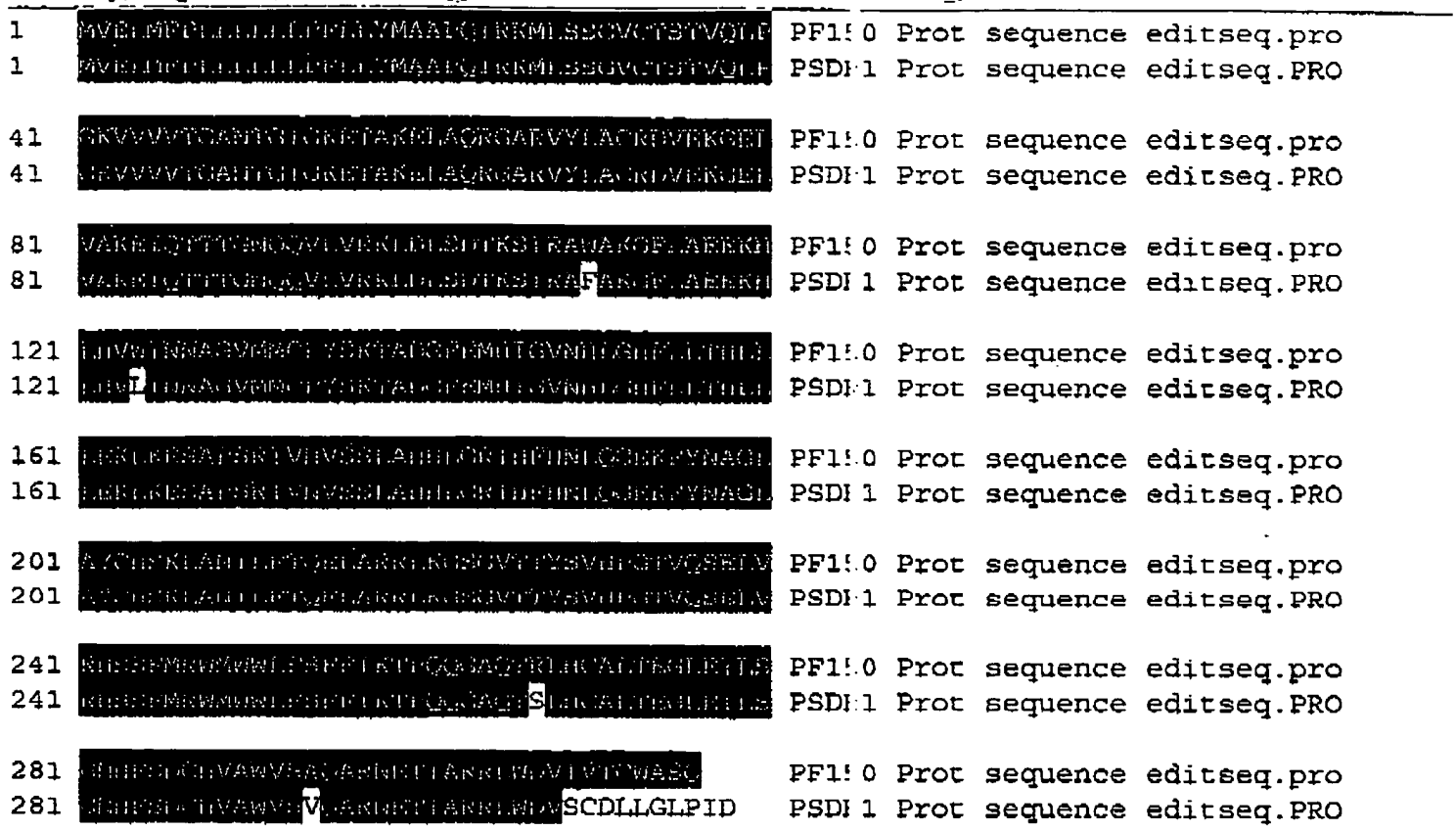

Decoration 'Decoration #1': Shade (with solid black) residues that match PF150 Prot sequence editseq.pro exactly.

Exhibit C